

2. LITERATURE REVIEW

2.1 Cancer

Cancer, the uncontrolled growth of cells, combines these cells and leads to the formation of extra mass tissue known as tumor (1). With 21.4 million new cases reported in 2021 and 11.6 million deaths, cancer is found to be the leading cause of death globally (2). Globally, nearly 1 in 5 deaths is due to cancer and approximately 70% of deaths from cancer occur in low- and middle-income countries. Cancer metastasis is defined as the formation of new tumors (secondary and tertiary tumor nests) in tissues and organs away from the primary site of tumor origin and these metastases account for a vast majority of morbidity and mortality of cancer patients and is associated with about 90% of all cancer-associated deaths (3, 4).

2.2 Breast Cancer

Breast cancer, the most commonly occurring cancer in women, comprises almost half of all malignancies in females. Figure 2.1 represents the most diagnosed cancer among female in 2020 and it can be clearly seen that females are suffering from breast cancer throughout the world including India (5, 6). Breast cancer is the leading cause of cancer-related death among females worldwide. In 2020, an estimated 2.8 million cases and 685,000 deaths occurred. Mortality rates are highest in the very young (less than age 32) and in the very old (greater than age 65). It comes into sight that the very young have more aggressive disease, and the very old may not be treated aggressively or may have co-morbid disease that increases breast cancer fatality (7).

Women from less developed regions (1.7 million cases) have slightly a greater number of cases compared to more developed (1.1 million cases) regions. In India, about 1,98,937 new cases of breast cancer were diagnosed and the number of women dying of breast cancer was 101,368. So, in India, for every 2 women newly diagnosed with breast cancer, one lady is dying because of breast cancer (8).

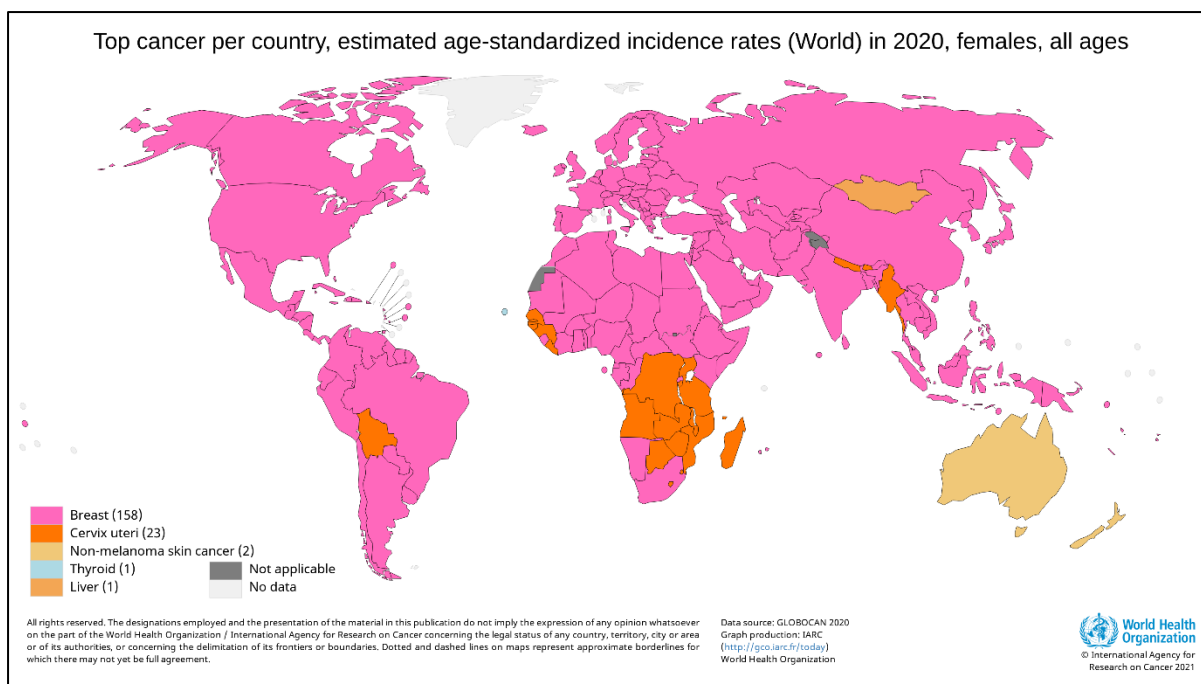


Figure 2.1 Most commonly diagnosed cancers, 2020 (Obtained from WHO, 2020)

2.2.1 Pathogenesis of breast cancer

Breast cancer is a malignant tumor that starts in the cells of the breast. Like other cancers, there are several factors that can raise the risk of getting breast cancer. Damage to the DNA and genetic mutations can lead to breast cancer have been experimentally linked to estrogen exposure. Some individuals inherit defects in the DNA and genes like the BRCA1, BRCA2 and P53 among others. Those with a family history of ovarian or breast cancer thus are at an increased risk of breast cancer (9-12).

The immune system normally seeks out cancer cells and cells with damaged DNA and destroys them. Breast cancer may be a result of failure of such an effective immune defence and surveillance. These are several signalling systems of growth factors and other mediators that interact between stromal cells and epithelial cells. Disrupting these may lead to breast cancer as well (13-15).

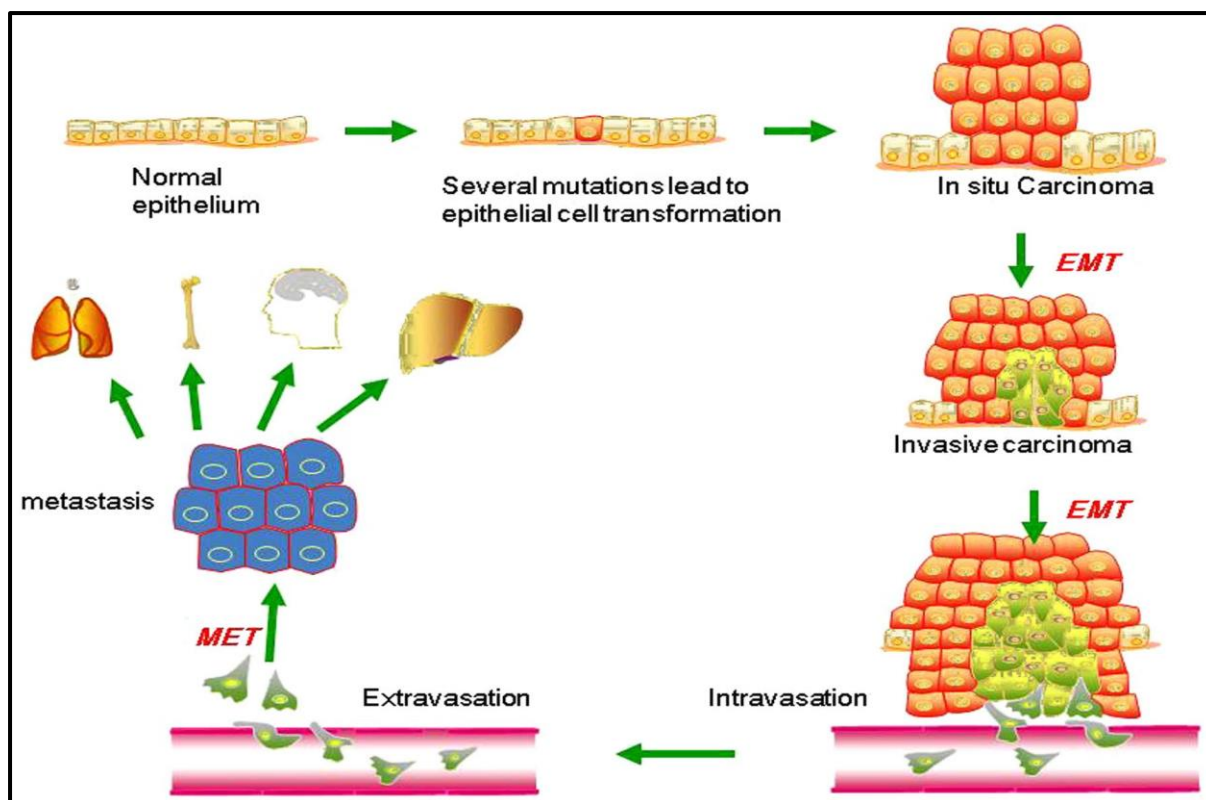


Figure 2.2 Pathogenesis of Breast cancer

2.2.2 Current treatment strategies

Though great strides have been made in the treatment of cancer over the past years, it continues to be a major health concern and, therefore, extensive efforts have been made to search for new therapeutic approaches. The conventional therapeutic approaches for cancer are surgery, chemotherapy, and irradiation; chemotherapy being an important component of treatment for cancer patients.

2.2.2.1 Conventional chemotherapy

The use of cytotoxic chemotherapy in both advanced and early-stage breast cancer has made significant progress in the last few years with several landmark studies identifying clear survival benefits for newer therapies. Despite improvements with better understanding of the use of adjuvant therapies for early-stage breast cancer, the treatment of metastatic disease remains a major challenge. The use of anthracyclines and taxanes in the adjuvant setting has led to an increasing number of women presenting with metastatic disease having already been exposed to these agents adding to the complexities of their management. Despite being incurable, metastatic breast cancer (MBC) often remains chemo-sensitive such that symptom

control and prolongation of survival can be achieved. However, response duration remains disappointingly short- and long-term survival remains uncommon (16-18).

2.2.2.2 Adjuvant Therapy

Early breast cancer is limited to the breast alone or, in the case of women with node-positive disease, the breast and loco regional lymph nodes, and all detected disease can be removed surgically (19). The delay in the initiation of chemotherapy post-surgery is no longer an issue due to improved surgical techniques. Chemotherapy is routinely commenced within six weeks of surgery if indicated. However, micro metastatic disease may remain either locally or at distant sites that, if left untreated, could over the coming years develop into a life-threatening clinical recurrence (20).

Over the past few years, thousands of women have been enrolled into various clinical trials addressing questions over the role of chemotherapy versus no chemotherapy, role of polychemotherapy versus single agents, role of anthracyclines versus no anthracyclines, role of doses and schedules, and more recently adding taxanes and other novel compounds in chemotherapy arms (21, 22). The most used standard adjuvant chemotherapy regimens are listed in Table 2.2.

Standard Regimes	Components
AC (w or w/o T)	Adriamycin, Cyclophosphamide, Taxol
CMF	Cyclophosphamide, Methotrexate, fluorouracil (5 – FU)
CEF	Cyclophosphamide, Epirubicin, fluorouracil (5 – FU)
CAF	Cyclophosphamide, Adriamycin, fluorouracil (5 – FU)

Table 2.2 Standard Adjuvant chemotherapy regimens

Polychemotherapy using an anthracycline-containing regimen has been the cornerstone of treatment for women without pre-existing heart disease who require adjuvant chemotherapy for breast cancer.

2.2.2.3 Chemotherapy for Metastatic Breast Cancer (MBC):

Although generally incurable, MBC remains chemo sensitive such that symptom palliation and prolongation of survival can be achieved. However, response duration remains disappointingly short- and long-term survival remains uncommon, such that ongoing research is required. Anthracyclines possess significant activity in chemo-naïve patients or those who received them in the adjuvant setting more than 12 months ago. Response rates of 30-40% have been

documented in patients with MBC (23). Despite their significant role in the adjuvant setting, the use of anthracyclines in patients with MBC may be limited by significant toxicity. For patients exposed to anthracyclines in the adjuvant setting or who have failed in the metastatic setting, taxanes based treatment is currently the standard of care. Capecitabine has demonstrated single agent activity in MBC, with a response rate more than 20% and median survival greater than 1 year even in patients with disease refractory to both anthracycline and taxanes, and with a favourable toxicity profile and oral bioavailability (24, 25).

Trastuzumab, in combination with chemotherapy has demonstrated a survival benefit over chemotherapy alone in patients with Her-2/neu expressing breast cancer. Trastuzumab in combination with either doxorubicin and cyclophosphamide or with paclitaxel achieved significantly greater time to progression, response rates, and 2-year survival compared to chemotherapy alone (26-28).

2.2.2.4 Limitations of Chemotherapy:

Despite the significant advances in cancer detection, prevention, surgical oncology, chemotherapy and radiation therapy, there is still no common cure for cancer. Chemotherapy is an effective treatment against cancer but undesirable chemotherapy reactions and the development of resistance to drugs which results in multi-drug resistance (MDR) are the major obstacles in cancer chemotherapy (29, 30).

✓ Lack of selectivity and undesirable side effects:

Conventional chemotherapy relies on the premise that rapidly proliferating tumor cells are more likely to be destroyed by cytotoxic agents than normal cells. However, these cytotoxic agents have little or no specificity, which leads to systemic toxicity causing undesirable side effects.

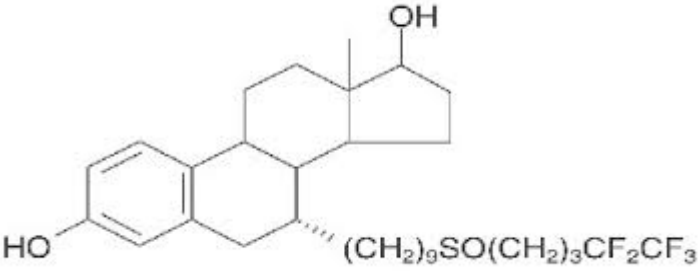
“We have met the enemy, and he is us,” a quote from the comic strip “Pogo” by Walt Kelly, summarizes the primary difficulty of treating tumors using chemotherapeutics, namely, that cancerous and normal cells are remarkably similar. Although cancer cells harbour mutated genes and resultant mutated proteins that affect cell division and/or contribute to oncogenesis, the tumor and normal cells share the same DNA and major metabolic pathways. Thus, traditional chemotherapeutic compounds that attack DNA replication or cell division in a cancer cell can also attack a normal dividing cell, resulting in serious side

effects such as neutropenia, anaemia, hair loss, damage to liver, kidney, bone marrow and gastrointestinal toxicity (31, 32).

✓ Multi drug resistance (MDR)

Apart from toxicity, chemotherapeutic drug resistance in cancer therapy further limits the usefulness of anticancer agent. Although the mechanism of drug resistance is not clearly understood, however the cancer drug resistance is mainly due to pump and non-pump resistances. Pump resistance is due to ATP binding cassette (ABC) transporters including over-expression of P-glycoprotein (P-gp), a multidrug resistance protein (33) that alter antitumor drug transport mechanisms, multidrug resistance-associated protein such as mutated Topoisomerase II which decrease drug activation and accelerate drug degradation where drug gets inactivated by conjugating with increased glutathione and ABC sub-family G member 2 (ABCG2), which expel drugs from cancer cells (34). In addition, non-pump resistance is mainly caused by overexpression of antiapoptotic proteins (B-cell lymphoma – 2 [BCL-2]) that prevent apoptosis in cancer cells (35).

2.3 Fulvestrant

Drug	Fulvestrant
Molecular formula	C ₃₂ H ₄₇ F ₅ O ₃ S
Molecular weight	606.8 g/mol
Molecular structure	
Bioavailability	Orally: 2.3 ± 0.3%, IM: 100%
Log P	9.2
BCS Class	Class IV
pKa	10.32
t _{1/2}	IV = 13.5 hours
Solubility	Soluble in Methanol (10 mg/ml), Ethanol (15 mg/ml), Tetrahydrofuran (30 mg/ml), Acetonitrile (14 mg/ml)

Elimination	Fulvestrant was rapidly cleared by the hepatobiliary route with excretion primarily via the faeces (approximately 90%). Renal elimination was negligible (less than 1%).
Melting Point	108°C – 112°C
Adverse drug reactions	Weight gain, thromboembolic problems, neutropenia, leukaemia, anaemia. Some fewer common side-effects observed are vulvovaginal dryness, pelvic pain, and vaginitis

Table 2.3 Drug Profile of Fulvestrant

2.3.1 Mechanism of action of Fulvestrant

Fulvestrant competitively and reversibly binds to estrogen receptors present in cancer cells and achieves its anti-estrogen effects through two separate mechanisms. First, fulvestrant binds to the receptors and downregulates them so that estrogen is no longer able to bind to these receptors. Second, fulvestrant degrades the estrogen receptors to which it is bound. Both mechanisms inhibit the growth of tamoxifen-resistant as well as estrogen-sensitive human breast cancer cell lines (36, 37).

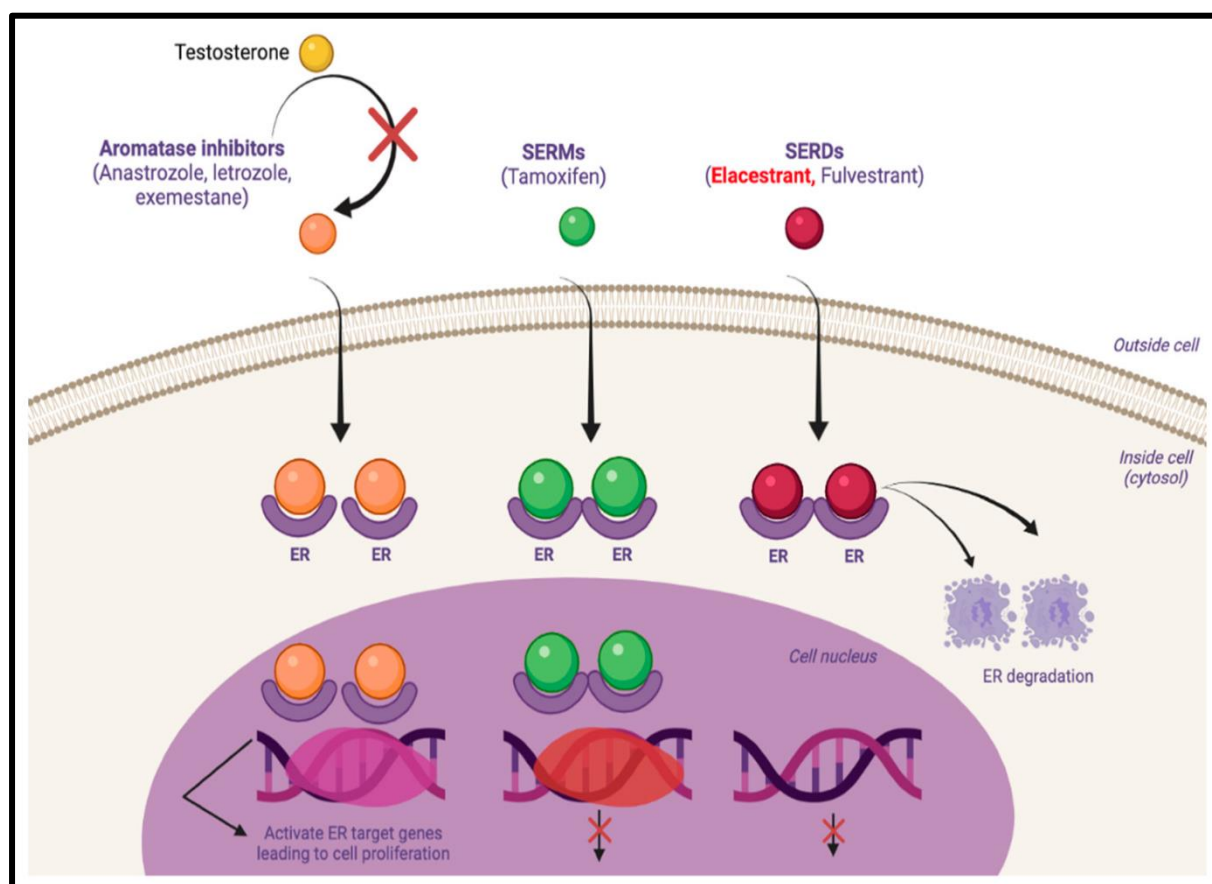


Figure 2.3 Representation of Fulvestrant mechanism of action

2.3.2 Drawbacks associated with Marketed formulation

Fulvestrant is practically insoluble in water. Hence, marketed formulation of Fulvestrant (Faslodex) is formulated using castor oil, ethanol, benzyl alcohol, benzyl benzoate in the form of intramuscular (IM) injection. Due the higher viscosity of formulation and oil present people suffer from hypersensitivity reactions, which mainly includes injection site pain (75%), headache (36%), back pain, hot flashes, muscle, joint and bone pain(38). Benzyl benzoate presents side effects such as loss of consciousness, scaling of skin and blister formation. Castor oil being vegetable oil is safe to use, but injection have adverse effects such as dizziness, diarrhoea, pelvic congestion and many more. Ethanol though being safe cause neutropenia on injection above 5% in systemic circulation (39).

2.3.3 Resistance to fulvestrant

Multidrug resistance (MDR) is the most frequent phenomenon by which cancer cells elude chemotherapy. Fulvestrant is second line agent given after resistance to tamoxifen in hormone receptor positive or estrogen receptor positive breast cancer. But due to constant mutation and genetic factors, resistance to fulvestrant is also seen in mostly 48% of people receiving hormonal therapy or fulvestrant therapy (40). Nevertheless, all patients with ER+ metastatic breast cancer treated with endocrine therapy will develop endocrine resistance eventually. In fact, ER+ breast cancer may either be unresponsive to endocrine therapy (de novo resistance) or lose endocrine responsiveness over time (acquired endocrine resistance). From a clinical perspective, de novo and secondary or acquired resistance are terms that have been arbitrarily defined. Given the heterogeneity in mechanisms of endocrine resistance, as well as an increasing number of targeted therapeutics that aim to revert such resistance. Several molecular mechanisms have been described as the drivers of resistance to treatment (41). The loss of ER expression, the development of *ESR1* mutations, and activation of several signalling pathways such as PI3K or MAPK are among the most relevant resistance mechanisms. This heterogeneity in the resistance (35) development is not only applicable to the progressing disease but can be also drug-specific. The overexpression of cyclin E2 and suppression of DAXX protein are two major markers to resistance of fulvestrant in patients (42).

2.3.4 Reported research

Hascicek C et al., developed fulvestrant polymeric nanoparticles using PEG – PCL as the polymer for intratumoral injection. They studied the influence of polymer hydrophobicity of two different polymeric nanomaterials with respect to invitro properties, cell cytotoxicity and

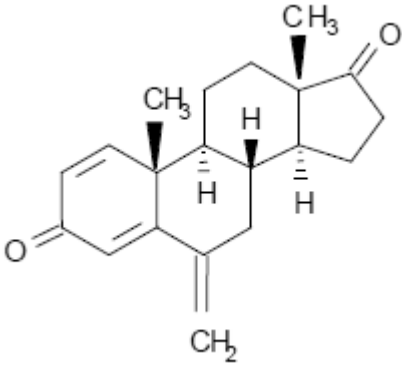
cell uptake potency. The nanoparticles were of negative charge and showed sustained release profile. The cell cytotoxicity data also supported the fact that hydrophobic polymer is required to increase the cytotoxicity of drug and to retain the drug for prolonged period. The major drawback with the developed formulation was its route of administration as intratumoral administration can be difficult and may present some sensitivity reactions (43).

Purohit P et al, developed orally bioavailable prodrug for treatment of metastatic breast cancer. The prodrug enhanced the systemic exposure upon oral administration and the bioavailability was improved up to 8.7 folds. The study of prodrugs on MCF – 7 cell lines showed substantial increase in anticancer activity. The tests on tumor xenograft model shows 48 – 88% reduction in tumor burden (44).

XIAN libang Medicine science and technology had developed a controlled delivery micro balloon for the sustained delivery of fulvestrant using PLA and PCL as a biodegradable polymer. The formulation was prepared using high shear homogenization method and the size was found between 15 to 125 μ and encapsulation of 80% (45).

Park J developed an implantable silastic tubing for local delivery of fulvestrant to breast tissues. The in vitro and in vivo results showed promising results where the antitumor activity was found to increase significantly to increased local concentration. The results supported the fact that local delivery can treat cancer rapidly (46).

2.4 Exemestane

Drug	Exemestane
Molecular formula	$C_{20}H_{24}O_2$
Molecular weight	296.17 g/mol
Molecular structure	
Bioavailability	Orally: $42 \pm 1.6\%$
Log P	3.7

BCS Class	Class IV
pKa	14.82
t _{1/2}	8.9 hours
Solubility	Soluble in Methanol (24 mg/ml), Ethanol (40 mg/ml), Tetrahydrofuran (18 mg/ml), Acetonitrile (31 mg/ml)
Absorption	40 % of oral exemestane is absorbed from GI tract, achieves peak plasma concentration within 1 – 2 hours, and absorption is increased by fatty meal; highly metabolized by first pass metabolism.
Elimination	Fulvestrant was rapidly cleared by the hepatobiliary route with excretion primarily via the faeces (approximately 90%). Renal elimination was negligible (less than 1%).
Melting Point	154°C – 158°C
Adverse drug reactions	Although generally well tolerated, exemestane is expected to cause or exacerbate hot flashes or intermittent flushing in some women; fatigue and mild nausea are common; vomiting, headache, and dyspnoea are uncommon; it is teratogenic and should not be used in premenopausal women

Table 2.4 Drug Profile of Exemestane

2.4.1 Mechanism of action of Exemestane

Breast cancer cell growth may be estrogen-dependent. Aromatase (exemestane) is the principal enzyme that converts androgens to estrogens both in pre- and postmenopausal women. While the main source of estrogen (primarily estradiol) is the ovary in premenopausal women, the principal source of circulating estrogens in postmenopausal women is from conversion of adrenal and ovarian androgens (androstenedione and testosterone) to estrogens (estrone and estradiol) by the aromatase enzyme in peripheral tissues(47). Estrogen deprivation through aromatase inhibition is an effective and selective treatment for some postmenopausal patients with hormone-dependent breast cancer(48). Exemestane is an irreversible, steroidal aromatase inactivator, structurally related to the natural substrate androstenedione. It irreversibly binds to the active site causing permanent inhibition necessitating de novo synthesis to restore enzymatic function. Exemestane significantly lowers circulating estrogen concentrations in postmenopausal women but has no detectable effect on the adrenal biosynthesis of corticosteroids or aldosterone. This reduction in serum and tumor concentrations of estrogen

delays tumor growth and disease progression. Exemestane has no effect on other enzymes involved in the steroidogenic pathway up to a concentration at least 600 times higher than that inhibiting the aromatase enzyme(49).

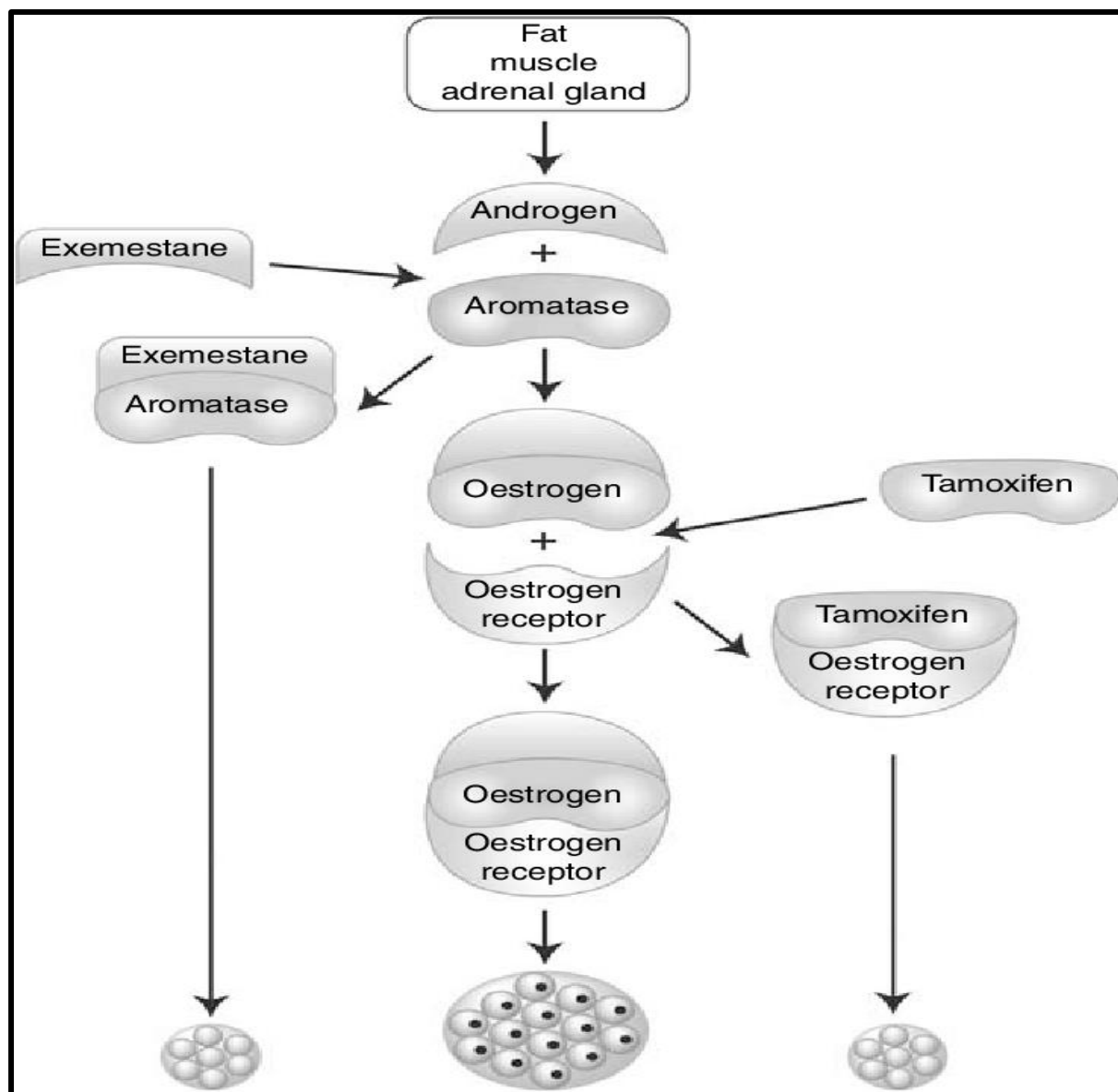


Figure 2.4 Mechanism of action of Exemestane

2.4.2 Problems associated with marketed formulation

Exemestane is a potent third generation steroidal aromatase inactivator used in the treatment of advanced breast cancer in postmenopausal women. The bioavailability of exemestane is limited to only 42% due to poor solubility and extensive first-pass metabolism and further the absorption is highly variable, which is dependent on formulation type and food. The current oral therapy with exemestane pose problems such as unpredictable dissolution and absorption,

poor patient compliance with common adverse effects such as body weight change, fatigue, dizziness, hot flushes, arthralgia, myalgias and osteoporosis.

2.4.3 Resistance to Exemestane Therapy

Resistance to AIs is divided into two main types: primary/*de novo* resistance and secondary/acquired resistance. Recently, ESO-ESMO international consensus guidelines for advanced breast cancer defined the primary resistance as a relapse during the first 2 years of adjuvant endocrine therapy or progression of disease within the first 6 months of first-line endocrine therapy for metastatic breast cancer. Secondary/acquired resistance is defined as a relapse while on adjuvant endocrine therapy but after the first 2 years, or as a relapse within 12 months of completing adjuvant endocrine therapy, or progression of disease after 6 months of initiating endocrine therapy for metastatic breast cancer. Although the clinical distinction between the two types of resistance is not yet well defined, the mechanisms underlying these two types of resistance are likely to overlap(50, 51). The main reason behind the acquired resistance to exemestane or aromatase inhibitors is estrogen related gene mutation (ESR1) mutation. Another reason behind resistance is postulated to be growth factor receptor expression and activation. The increase in HER2 activation leads to a ligand-independent activation of ER through MAPK phosphorylation on S118, inducing acquired resistance to AIs.

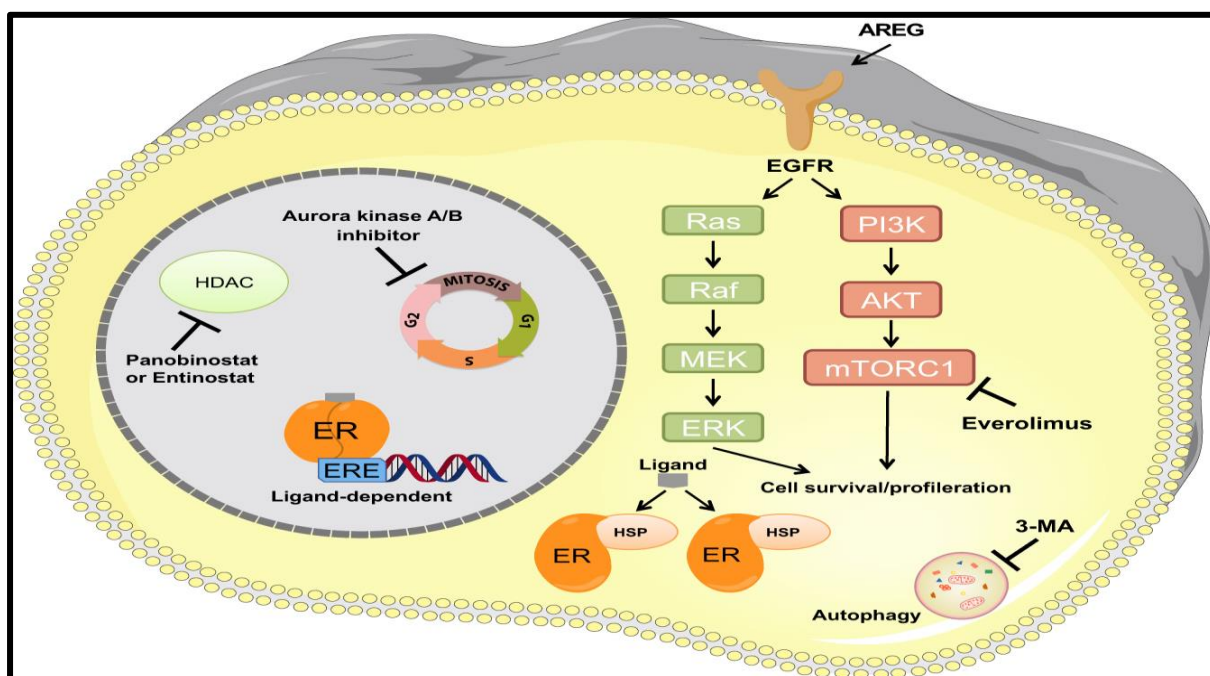


Figure 2.5 Acquired resistance to aromatase inhibitors (Exemestane)

2.4.4 Reported research for exemestane

Sr. No	Formulation	Outcomes	Ref No.
1	Self-Micro Emulsifying Drug Delivery Systems (SMEDDS)	An optimized exemestane loaded formulation was prepared using Capryol 90 and Cremophor EL, that showed good solubilization and improved bioavailability.	(52)
2	Oral Proliposomes	Exemestane Proliposomes with aim to improve oral bioavailability by means of solubility enhancement, and permeability enhancement using DSPC and DMPG as lipids.	(53)
3	Transdermal Proliposomes	Exemestane Proliposomes for transdermal delivery with aim to improve the bioavailability by bypassing the first pass metabolism. The bioavailability was increased by 2.4 times and invitro drug release followed zero order kinetics.	(54)
4	Polymer Lipid nanoparticles	The polymer lipid nanoparticles were prepared using PCL as polymer and P90G as lipid. The nanoparticles were prepared by nano precipitation method. The formulation showed controlled release and in vitro cytotoxicity studies displayed improved activity against MCF – 7 cell lines	(55)
5	Freeze Dried Solid Dispersion	Freeze dried solid dispersion for exemestane with Phospholipon 80H and sodium deoxycholate and 10% HP β CD for lyophilization. In vivo Pharmacokinetic studies showed 2.3-fold increase in AUC and improved solubility and dissolution rate.	(56)
6	Solid Dispersion	Lipid based solid dispersions were prepared using Gelucire 44/14 as surfactant and vitamin E TPGS as lipid. Exemestane converted to amorphous form from crystalline form. The permeability of drug was improved.	(57)
7	Inclusion complexes	The oral bioavailability of exemestane was found to be 5% due to limited solubility and first pass effect. HP β CD and ME- β CD inclusion complexes were formulated for improved solubility and permeation of exemestane. The permeation study showed 3-fold increase.	(58)
8	Cubosome gel	The liquid lyotropic crystalline gel (Cubosome) were prepared using GMO and Pluronic F127 by high shear homogenization method. The formulation	(59)

		when studied for in vitro cell cytotoxicity study presented 4-fold increase on MDA MB 231 cells. The permeation studies also showed improved permeation.	
9	Sodium Alginate Nanoparticles	The sodium alginate nanoparticles were prepared by controlled gelation method. The results of in vitro study showed the controlled release.	(60)
10	Polymeric Nanoparticles	The PLGA/MMT nanoparticles were prepared by modified solvent extraction/evaporation technique, using vitamin E TPGS as emulsifier. The MCF – 7 cell line showed improved cytotoxicity efficiency compared to exemestane solution.	(61)
11	Self-Nano Emulsifying Drug Delivery Systems	The SNEDSS of Exemestane with aim to improve the permeability of drug were prepared using Imwitor 988, Kolliphor RH40 and Labrasol. The drug loading was found to be 15mg/g and the permeability study on the porcine skin showed that permeation of drug was twice as compared to the drug itself.	(62)

Table 2.5 Reported work on exemestane

2.5 Nanotechnology in cancer therapy

The intrinsic limits of conventional cancer therapies prompted the development and application of various nanotechnologies for more effective and safer cancer treatment as nanotechnology has the potential to revolutionize cancer diagnosis and therapy (63). The increasing interest in applying nanotechnology to cancer treatment is attributable to its outstandingly appealing features for drug delivery, diagnosis and imaging, synthetic vaccine development and miniature medical devices, as well as the therapeutic nature of some nanomaterials themselves (64). Distinctive features of nanotechnology in oncological applications are as follow:

- ✓ Improvement of the drug therapeutic index by increasing efficacy and/or reducing toxicities
- ✓ Targeted delivery of drugs in a tissue-, cell- or organelle-specific manner
- ✓ Enhancement of the pharmaceutical properties (for example, stability, solubility, circulating half-life and tumour accumulation) of therapeutic molecules
- ✓ Enabling of sustained or stimulus-triggered drug release
- ✓ Facilitation of the delivery of bio macromolecular drugs (for example, DNA, small interfering RNA (siRNA), mRNA and protein) to intracellular sites of action

- ✓ Co-delivery of multiple drugs to improve therapeutic efficacy and overcome drug resistance, by providing more precise control of the spatiotemporal exposure of each drug and the delivery of appropriate drug ratio to the target of interest
- ✓ Transcytosis of drugs across tight epithelial and endothelial barriers (for example, gastrointestinal tract and the blood–brain barrier)
- ✓ More sensitive cancer diagnosis and imaging
- ✓ Visualization of sites of drug delivery by combining therapeutic agents with imaging modalities, and/or real-time feedback on the in vivo efficacy of a therapeutic agent
- ✓ Provision of new approaches for the development of synthetic vaccines
- ✓ Miniaturized medical devices for cancer diagnosis, drug screening and delivery
- ✓ Inherent therapeutic properties of some nanomaterials (for example, gold nanoshells and nanorods, and iron oxide nanoparticles) upon stimulation

Nanotherapies that incorporate some of these features (for example, improved circulation and reduced toxicity) are already in use today, and others show great promise in clinical development, with definitive results expected soon. Several therapeutic nanoparticle (NP) platforms, such as liposomes, albumin NPs and polymeric micelles, have been approved for cancer treatment, and many other nanotechnology-enabled therapeutic modalities are under clinical investigation, including chemotherapy, hyperthermia, radiation therapy, gene, or RNA interference (RNAi) therapy and immunotherapy.

2.6 Polymer Lipid Hybrid Nanocarriers

Among all the nanocarriers liposomes and polymeric nanoparticles have been most widely researched as novel strategy for delivery of variety of therapeutics including genetic materials due to their biocompatibility and in-vivo drug targeting. Hence both nanocarriers possess few shortcomings, it is prerequisite to superimpose these shortcomings with each other's advantage (65). Polymeric nanoparticles are a class of artificial vesicles which is made from synthetic amphiphilic block copolymers. They possess key attributes such as long-term stability and tuneability but are generally lacking in inherent biocompatibility and potential toxicity of long-term accumulation of synthetic molecules in the body. The liposome is a closed vesicle composed of a lipid bilayer membrane and readily used for the functional reconstitution of integral membrane proteins (66). The biocompatible, non-denaturing interface of liposomal capsules also makes this a suitable material for encapsulation and isolation of biomolecules. Unfortunately, the lack of long-term stability of liposomes can be problematic for applications

which require extended shelf lives or prolonged monitoring times. In addition, membrane specific interactions with various molecules in the host media can acutely perturb the structural integrity of liposomes so there is an ample room to develop such a hybrid delivery system which bring together the excellent mechanistic stability and chemical tunability of polymeric nanoparticles with inherent biocompatibility and bio-functionality of liposomes (67).

2.6.1 Types of polymer lipid hybrid nanocarriers

Type	Description	Synonyms
Polymer core-lipid shell (68)	Colloidal supramolecular assemblies consisting of polymer particles coated with lipid layer (s)	Lipoparticles Lipid-polymer particle assemblies Lipid-coated NPs Nanocell Polymer-supported lipid shells
Core-shell-type hollow lipid-polymer-lipid NP (69)	Hollow inner core surrounded by concentric lipid layer, followed by polymeric layer, again followed by lipid layer along with lipid-PEG.	
Erythrocyte membrane-camouflaged polymeric NPs (70)	Sub-100-nm polymeric particles are coated with RBC membrane derived vesicles to mimic complex surface chemistry of erythrocyte membrane	Biomimetic NPs

Monolithic LPHNs	Lipid molecules are dispersed in a polymeric matrix	Mixed lipid-polymer particles
Polymer-caged liposomes (71)	These systems are composed of polymers, anchored or grafted at the surfaces of the liposomes to provide stability	

Table 2.6 Types of polymer lipid hybrid nanocarriers

2.6.2 Advantages of PLHNCs

PLHNCs has advantages of both liposomes and polymeric nanoparticles. Some extraordinary advantage performed by PLHNCs are listed here. (72, 73)

- ✓ The solid core made up of polymer acts as a cytoskeleton that provides mechanical stability, controlled released morphology, narrow size distribution, and higher availability of specific surface area.
- ✓ The outer lipid coat that encapsulates the polymeric core is biocompatible in nature and mimics the characteristic of cellular membranes. The lipid shell can interact with a huge variety drugs and indigenous molecules and surface can be modified for efficient targeting.
- ✓ Improved encapsulation of hydrophobic drugs with effective drug entrapment efficiency and drug loading has been reported for several drugs compared to liposomes or polymeric nanoparticles.
- ✓ Amphiphilic character of lipids facilitates the adsorption of hydrophilic compounds on the bilayer surface and insertion of hydrophobic molecules into the hydrophobic lamellar region. This feature allows PLHNCs to entrap and deliver multiple hydrophilic and hydrophobic therapeutic agents simultaneously.
- ✓ Optimization of the core and shell can result in tunable and sustained drug release profiles.
- ✓ PLHNCs exhibit storage and serum stability over prolong period.

- ✓ Besides passive targeting of PLHNCs based on particle size, they can be conjugated with appropriate targeting ligands such as aptamers, folic acid, transferrin, anti-carcinogenic embryonic antigen half-antibody, or single chain tumor necrosis factor to deliver PLHNCs at the target tissues for treating cancers.
- ✓ Particles smaller than 100 nm (similar to virus-like architecture) are promising for intracellular drug targeting and vaccine adjuvants.

2.6.3 Methods for preparation of PLHNCs

The Methods used to prepare PLHNCs broadly fall into two categories: the two-step method and the single-step method (74).

2.6.3.1 Two-step method

Polymer core is prepared separately using methods used to prepare polymeric nanoparticles and lipid layer is prepared separately mimicking liposome preparations. Then two different assemblies are mixed up using process i.e., Ultrasonication, direct hydration, homogenization, and extrusion to obtain desired sized polymeric core-lipid shell nanocarriers (75). Representation of two step method is shown in figure 2.6.

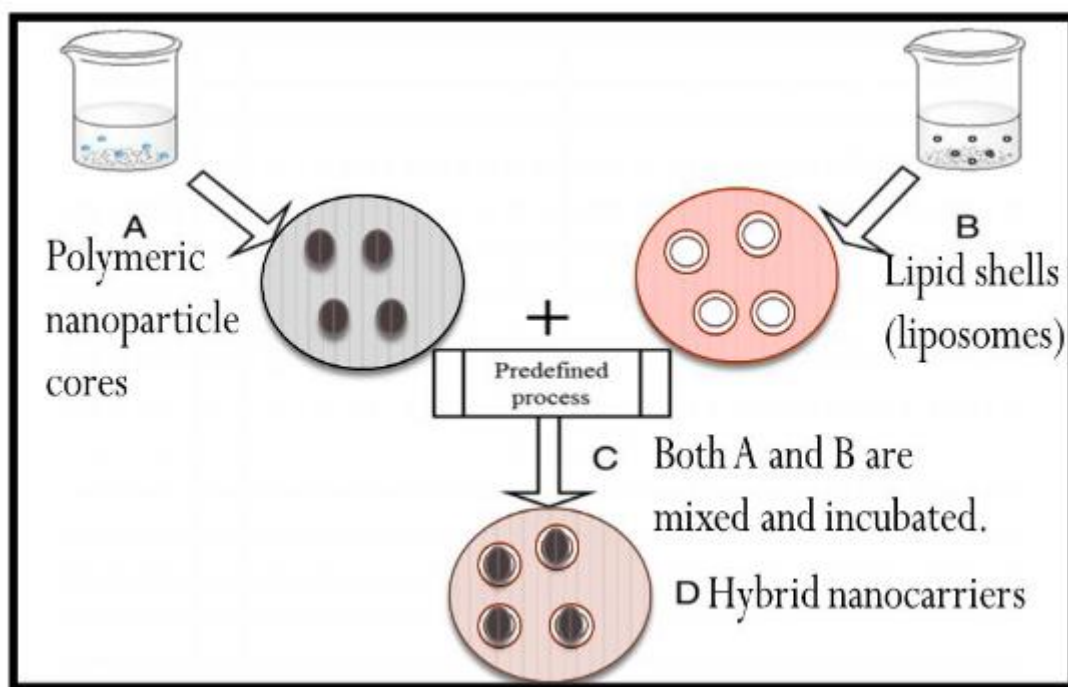


Figure 2.6 Two-step method PLHNCs

2.6.3.2 Single step method

Single step method is relatively more used as it combines both steps at the same time. It is work on the principle of the self-assembly. Single step method is further divided in to two approaches.

2.6.3.2.1 Modified solvent evaporation method

Briefly, the block copolymer along with hydrophobic drug have been dissolved in immiscible mixture of water with any organic solvent i.e., DCM (dichloromethane), chloroform, or even ethyl acetate. A fixed quantity of lipid has been dispersed in double distilled water with help of bath sonication, heat and/or mechanical stirring. Then organic phase has been mixed with aqueous phase with continuous stirring (76). Tiny droplets formed of the organic phase has been solidifies in the form of nanoparticles which has outer coating of lipid membrane. Extra organic solvent is then evaporated by overnight stirring or by incubating in vacuum desiccator (75).

2.6.3.2.2 Single step nano-precipitation

n single step nano-precipitation, polymer along with hydrophobic drug(s) have been solubilized in water miscible solvent i.e., ACN (acetonitrile) or Acetone. Then organic phase was added drop by drop in a controlled manner to aqueous phase containing lipid or combination of lipids. The resulting mixture was vortexed and homogenised or ultrasonicated to achieve desired particle size, most probably in nanoscale (77). The alteration between both the single step methods have been displayed in figure 2.7.

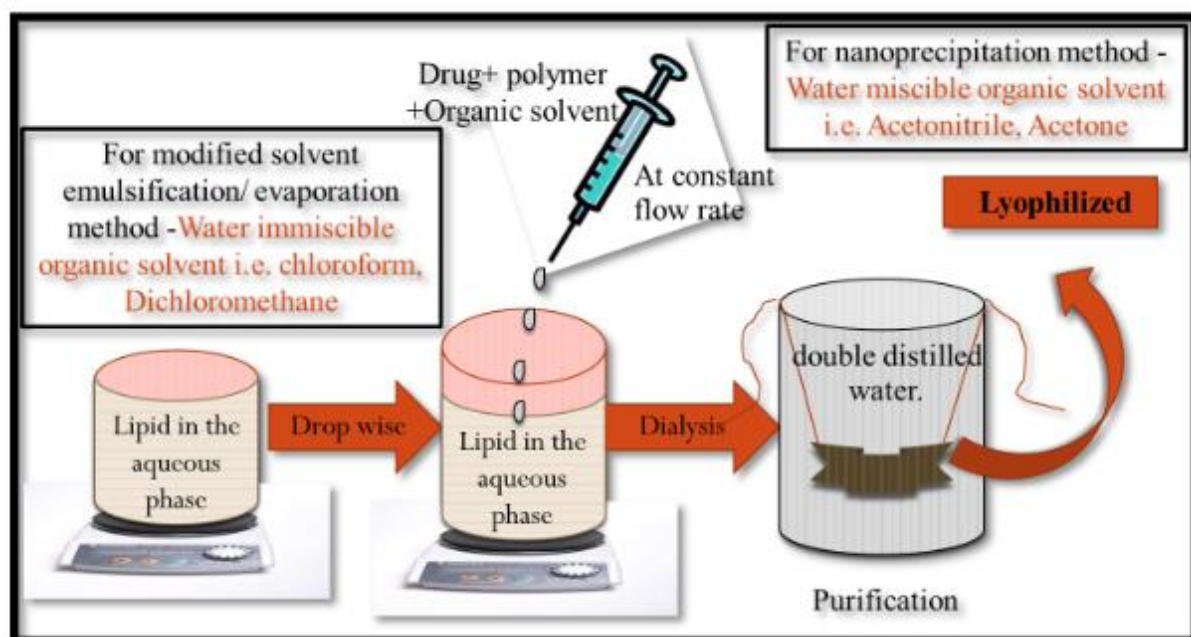


Figure 2.7 Single step method

2.6.4 Recent literature of polymer lipid hybrid nanocarriers

Drug	Polymer	Lipid	Particle size	EE/DL	Application	Ref
Doxorubicin and Combretastatin	PLGA	PC/Chol/DS/PE-PEG	180 – 200 nm	NA	Melanoma Lewis lung cancer	(78)
Doxorubicin	PLGA	DEPE-PEG Lecithin	118.7±0.7 5 nm	45.76± 6.58 %	Folate receptor mediated drug delivery of anti-cancer agent, doxorubicin, resulted in higher cell internalization	(79)

					and enhanced cell-killing effect toward MCF-7 cells with a significantly lower IC50.	
Docetaxel	PLGA	Lecithin PEG	70 – 80 nm	59±4.5 %	Docetaxel loaded Hybrid nanoparticle exhibited 20 hours as T50. These carriers also exhibited good stability in 10% bovine serum albumin and in 10% plasma solution.	(80)
Paclitaxel	PLGA	Soybean lecithin D-α-	120 – 150 nm	>80	Developed carriers provided	(81)

		tocopherol polyethylene glycol 1000 succinate (TPGS)			sustained release up to 8 days with a high tumor targeting potential through EPR effect. It also showed superior antitumor efficacy by inhibiting 58.8% volume of tumor at day 28.	
Docetaxel	PLGA	DSPE – PEG ₂₀₀₀	263.6 nm	66.88 %	Folic acid conjugation increased 38.2% for 0.5 hour incubation and 54% increase for 2 hours incubation	(82)

					during cell uptake study. Cell viability studies showed that formulation was 93.65% more effective than commercial preparation Taxotere	
Paclitaxel	PLGA	Soybean lecithin 1,2-Distearoyl-sn-glycero-3-phosphoethanolamine (DSPE-PEG)	186.9±8.5 2	81.34± 3.41	More drug reaches target site crossing Blood brain barrier and survival time for mice was PtxR-FPLNs (42 days), Ptx-FPLNs (38 days) compared	(83)

					to PtxR (18 days) and Paclitaxal (14 days)	
Melatonin	PLA	Didodecyl dimethylammonium bromide (DDAB) Cetyltrimethylammonium bromide (CTAB)	180 – 218 nm	90.35%	Coating with cationic lipids provides sustained and prolonged drug release, a pronounced benefit in ophthalmic application	(84)
Curcumin	PLGA	DPPC DSPE-PEG ₂₀₀₀	171.6±8.2	NA	By treating the metastatic breast cancer cells with the lipid-polymer hybrid nanoparticles of Curcumin decreased	(85)

					the adhesion onto tumor necrosis factor by 70% in capillary flow.	
Docetaxel	PLA	Chitosan	208-255.7 nm	75.9	PLA/chitosan nanoparticles provide rapid initial release of 40% drug in 5 hours and 70% cumulative release in 24 hours.	(86)
Doxorubicin	Chitosan	Hyaluronic acid	264 ± 2.2 nm	97.8 ± 1.3%	It is used to deliver anticancer drugs which results in enhanced circulation half-	(87)

					life and reduce the elimination of drug	
Docetaxel	PLGA	DSPE-PEG	110 ± 13.5 nm	77.65 ± 0.57%	The system increases the cellular uptake of docetaxel 2.5 folds and anti-proliferative activity 2.69–4.23 folds.	
Erlotinib	PLGA	DEPE-PEG2000 Dipalmitoyl phosphatidyl choline (DPPC) N-[1-(2,3-Dioleoyloxy)propyl]-N,N,N-trimethylammonium methylsulphate (DOTAP)	161 – 271 nm	77.18 %	Erlotinib loaded Core Shell Lipid Polymer Hybrid Nanoparticles demonstrated 170 nm size with 66% Entrapment efficiency and greater	(88)

					uptake and efficiency in A549 cells.	
--	--	--	--	--	--	--

Table 2.7 Recent literature on development of polymer lipid hybrid nanocarriers

EE: Entrapment Efficiency; DL: Drug Loading; NR: Not Reported; HPESO: Hydrolysed Polymer of Epoxidized Soyabean Oil; MDR: Multi-Drug Resistant; PLGA: Poly(Lactic-co-Glycolic Acid); DLPC: Dilinoleoylphosphatidylcholine; DMPE- DTPA: 1,2-ditetradecanoyl-sn-glycero-3 phosphoethanolamine-N- diethylenetriaminepentaacetic acid; DSPE-PEG, 1,2-distearoyl-sn glycero-3- phosphoethanolamine-N-[amino(polyethylene glycol)]; PMOXA-PDMSPMOXA, poly(2-methyloxazoline)-block-poly(dimethylsiloxan)-block-poly (2-methyloxazoline); DPPC, dipalmitoyl phosphatidylcholine; PEI, polyethyleneimine; EPC, 1,2-dimyristoleoyl-sn-glycero-3-ethylphosphocholine; PGA, poly(glutamic acid); DPTAP, 1,2-dipalmitoyl-3-trimethylammonium-propane; PLA, poly(lactic acid); OQLCS, octadecyl-quaternized lysine- modified chitosan; DHA, cis-4,7,10,13,16,19-docosahexanoic acid; PBAE, poly-(β -amino ester).

2.7 Mesoporous Silica Nanoparticles (MSNs)

Mesoporous materials have known a great development since their discovery in the early 1990s by Kuroda et al. and by the Mobil Oil Company. The unique characteristics of periodic mesoporous materials with very large specific surface areas usually above $1000 \text{ m}^2 \text{ g}^{-1}$, well-defined mesopores of controlled size ($2 \text{ nm} \leq \text{size} \leq 20 \text{ nm}$) and morphology are obtained owing to the use of assemblies of amphiphilic organic molecules as pore-forming agents and structure-directing agents, which ensure the formation of ordered hybrid organic-inorganic mesophases as precursors of the inorganic porous structures. Due to their very interesting surface properties, mesoporous materials have found a great utility in different domains such as catalysis, separation, adsorption, sensor technology, gas storage, nanocasting, chromatography, and medicine (89-91).

Since 2001, when Vallet-Regí et al. introduced for the first time MCM-41 as a drug delivery system, much effort has been devoted to the design of versatile MSNs for treating diverse pathologies, with special emphasis in cancer treatment (Figure 2.8). Their high drug loading

capability, the possibility to attain localized and even combined therapy make them promising alternatives to develop advanced nanotherapeutics (92).

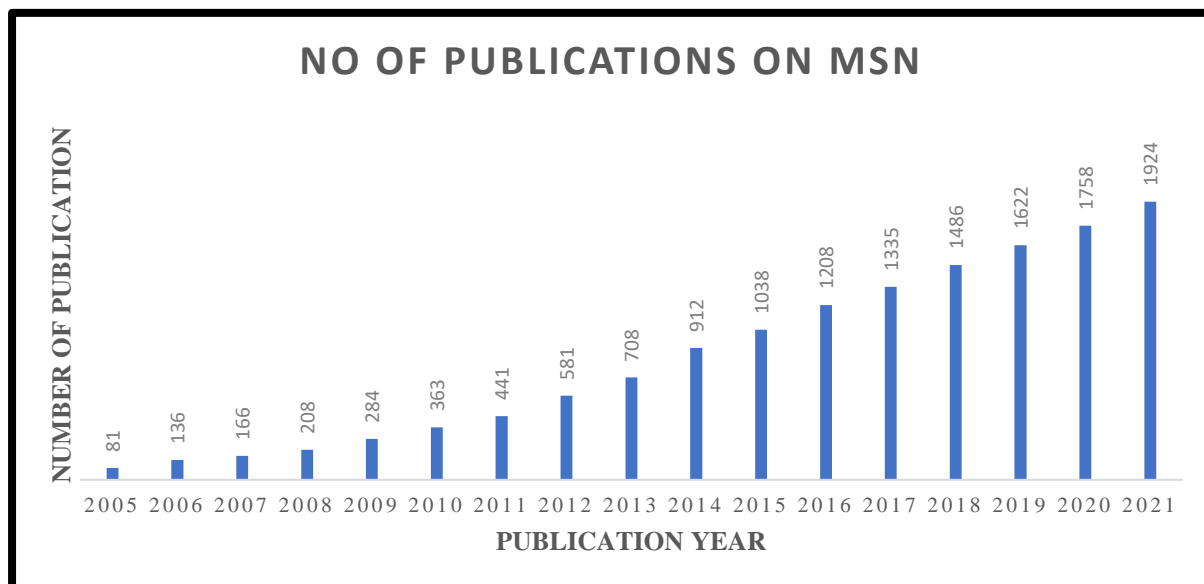


Figure 2.8 Number of publications per year indexed in the ISI Web of Science on the topic of “mesoporous” and “silica” and “drug” and “delivery” up to 2021.

Compared to other metal oxides such as titania and iron oxide, silica is considered to have better biocompatibility and can be safely taken up by living cells through endocytosis. The abundant presence of silanol groups in silica can have an affinity to phospholipids, which can be actively taken up by the cells. Additionally, its active surface property allows developing MSN with various surface properties through surface functionalization with different molecules, which consequently allows targeted delivery of different types of therapeutic agents. Due to its strong Si–O bond, silica nanoparticles are more stable to external stimuli such as mechanical stress and degradation compared to liposomes and dendrimers, eliminating the need for any additional stabilization such as covalent linkers used in other delivery systems (93-95).

2.7.1 Synthesis of Mesoporous Silica Nanoparticles (MSNs):

The synthesis of ordered mesoporous silica usually consists of several steps. Two different mechanisms are found to be involved for the formation of MSNs:

- ✓ True liquid-crystal templating (TLCT) in which the concentration of the surfactant is so high that under the prevailing conditions (temperature, pH) a lyotropic liquid-crystalline

phase is formed without requiring the presence of the precursor inorganic framework materials (normally tetraethyl- (TEOS) or tetramethyl orthosilicate (TMOS)).

- ✓ On the other hand, it is also possible that this phase forms even at lower concentrations of surfactant molecules, for example, when there is cooperative self-assembly of the structure directing agent (SDA) and the already added inorganic species, in which case a liquid-crystal phase with hexagonal, cubic, or laminar arrangement can develop (Figure 2.9).

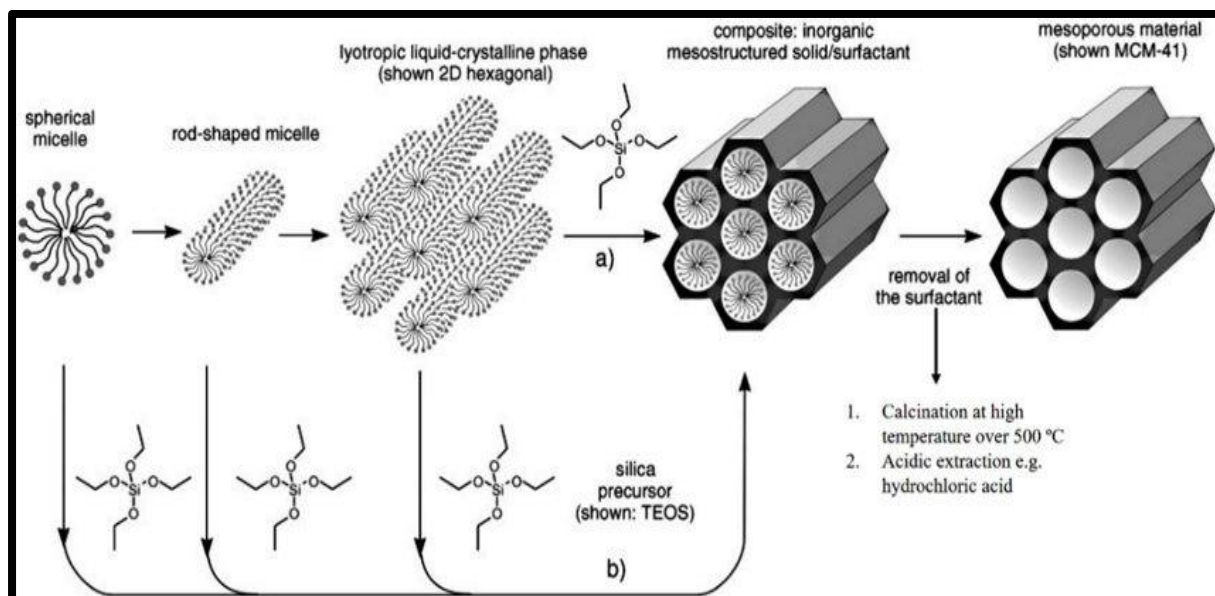


Figure 2.9 Formation of mesoporous materials by structure-directing agents: a) true liquid-crystal template mechanism, b) cooperative liquid crystal template mechanism.

In the meantime, the original approach has been extended by several variations, for example, using triblock copolymer template under acidic conditions by which means the so-called Santa Barbara amorphous (SBA) silica phases may be synthesized. Table 2.8 represents different types of mesoporous silica nanoparticles synthesized till date using different surfactants.

Label	Origin/name	Surfactant	Structure	Ref.
MCM – 41	Mobil composition of matter – 41	Alkyl trimethyl ammonium salt $C_nH_{2n+1}N+(CH_3)_3X^-$ (with $n = 12, 14, 16$ or 18 and $X = Cl$ or Br)	$P6mm$, hexagonal	(96)
MCM – 48	Mobil composition of matter – 48	Alkyl trimethyl ammonium salt $C_nH_{2n+1}N+(CH_3)_3X^-$	$Ia3d$, cubic	(97)

		(with n = 12, 14, 16 or 18 and X = Cl or Br)		
FSM – 16	Folder sheet mesoporous	Alkyl trimethyl ammonium salt $C_nH_{2n+1}N^+(CH_3)_3X^-$ (with n = 12, 14, 16 or 18 and X = Cl or Br)	P6mm, hexagonal	(98)
HMS	Hexagonal mesoporous silica	Uncharged amine surfactant $C_nH_{2n+1}NH_2$	Wormhole framework structure	(99)
SBA – 15	Santa Barbara amorphous	P123	P6mm, hexagonal	(100)
SBA – 16	Santa Barbara amorphous	PF127	Im3m, cubic	(101)
KIT – 6	Korea Advanced Institute of Science and Technology	P123	Ia3d, cubic	(102)
FDU – 1	FuDan University	Poly(ethylene oxide)– poly(butylene oxide)– poly(ethylene oxide) triblock copolymer B50-6600 (EO39BO47EO39, Dow Chemicals)	Fm3m, cubic	(103)
COK – 12	Centrum voor Oppervlaktechemie & Katalyse	P123	P6mm, hexagonal	(104)

Table 2.8 Different types of mesoporous silica, type of surfactant used, crystallographic structure.

A fundamental condition for the synthesis of MSNs is an attractive interaction between the template and the silica precursor to ensure inclusion of the structure director without phase separation taking place. Thus, the synthesis of MSNs involves mainly two reactants: Structure directing agents (template/surfactant) and silica source (105).

2.7.1.1 Structure Directing Agent:

Utilization of surfactant self-assemblies to direct the silica mineralization process is the most studied route towards the synthesis of highly ordered mesoporous silica. The general idea of using amphiphilic molecules as templates is since such systems can simultaneously form a hybrid surfactant/silica interface and self-assemble into robust and regular superstructures. Surfactants which are commonly used in the synthesis of OMS are frequently classified according to the nature of the interactions between their polar group and the hydrolysed silica precursors (106, 107). Cationic surfactants are efficient directing agents owing to the strong ionic interactions between their cationic head-group and the negatively charged silica precursors under basic conditions (synthetic route $S^+ I^-$ where S^+ = surfactant cations and I^- = inorganic precursor anions).

Utilization of neutral alkylamines was also demonstrated under neutral pH conditions. In this case, the synthesis mechanism relies on the formation of H-bonds between primary amines and neutral inorganic species (synthetic route $S^0 I^0$, where S^0 = non-ionic surfactants and I^0 = neutral silica species). Stabilization of the hybrid interface is also possible via the formation of H-bonds between the silicic acid and the ether oxygens of a PEO chain of non-ionic surfactants (synthetic route $S^0 I^0$ or $S^0 H + X^- I^+$ under strong acidic conditions, where X^- = inorganic counter ions such as Cl^- , Br^- , I^- , SO_4^{2-} or NO_3^-). The higher molecular weight and the wide variability in size and composition of this family of surfactants (that includes the commercial oligomeric acid alkyl- PEO, alkyl-phenol-PEO, sorbitan ester and PEO-based block copolymers) considerably extend the range of accessible pore size as well as the diversity of mesopore structures attainable (108-110).

A last synthetic route consists in using surfactants with an anionic polar head under basic conditions. The charge matching effect is ensured by the addition of cationic amino groups of organoalkoxysilanes to the reaction mixture (synthetic route $S^- N^+ + I^-$, where S^- = anionic surfactants, I^- = silicate species and N^+ = cationic amino groups).

The choice of alkylated quaternary ammonium salts to synthesize the first ordered mesoporous silica was motivated by their similarities with the ammonium salts commonly used as molecular templates in the synthesis of zeolites. The first ordered mesoporous alumino-silicates synthesized by Mobil scientists in 1992 were achieved in basic solution by using the cationic surfactant CTAB through the (S+I-) synthetic pathway. The synthesis was achieved under hydrothermal conditions with temperatures ranging from 100°C to 150°C. Well-ordered

mesoporous silica were then produced with the same quaternary ammonium-base cationic surfactants under acidic conditions (the S+X- I+ synthetic route where S+ = cationic surfactants, I- = silicate species and X- = inorganic counterions such as Cl⁻, Br⁻, I⁻, SO₄²⁻ or NO₃⁻). This acidic route presents the advantage of shorter synthesis time and lower surfactant concentrations. Furthermore, synthesis under acidic conditions could be achieved at room temperature (111).

The utilization of neutral primary amines for the synthesis of hexagonal mesoporous silica in 1995 was the first example of a neutral synthesis route S⁰T⁰. Advantageously, syntheses by using neutral alkylamines are performed under mild pH conditions, avoiding the addition of a high amount of mineral base (NaOH) or acid (HCl). Furthermore, this route makes possible the easy and efficient removal of the template (112).

PEO-based non-ionic surfactants such as polymeric (Pluronic P123 and F127 respectively) and Tween surfactants (ethoxylated derivatives of fatty esters of sorbitan) enabled the synthesis of highly ordered silica phases in relatively dilute aqueous solution. A highly acidic pH is yet required to generate the long-range organic–inorganic coulombic interactions at the start of the cooperative assembly process (113).

2.7.1.2 Silica source:

Development of sustainable strategies for the synthesis of ordered mesoporous silica implies the careful choice of silica precursor. Table 2.9 represents the comparison of different silica sources with their advantages and disadvantages.

Origin	Type	Advantages	Drawbacks	Ref
Synthetic	Silicon alkoxides (TEOS, TMOS)	Homogeneous silicate oligomers composition in solution Suitable for syntheses of highly organized mesostructures at any pH	Energy-intensive and expensive synthesis procedures Synthesized from toxic precursors Require the use of catalysts Soluble in organic solvents only Release of alcohols during the	(114)

			hydrolysis/condensation process	
	Soluble silicates (sodium silicate solution, colloidal silica, fumed silica)	Cheap Simple synthesis procedure Soluble in water	Silicate solutions composed of a variety of silicate oligomers with different degrees of polymerization Inorganic polycondensation difficult to control under neutral and acidic pH	(115)
Natural	Natural clays, diatomaceous earth, natural zeolites, other natural silica-containing minerals, Gramineae plants (rice husk)	Abundant, Cheap Non-toxic Possibility of forming mesoporous materials without the addition of organic surfactants: by taking advantage of metal cation impurities (K ⁺) or residual natural organic molecules (lignin)	The same drawbacks as soluble silicates Strong acids and high temperatures are used for purification	(116)
Recycling	Industrial wastes (coal ash, rice husk ash), electronic wastes (packaging resin), domestic wastes (glassware),	Abundant, Cheap and non-toxic Additional functionality (acidity) conferred by the residual	Slightly lower surface area and pore volume than with synthetic precursors	(117)

	regeneration of porous silica materials (hard templates used for nanocasting)	metal ions included within the silica matrix an answer to the problem of waste disposal		
--	---	---	--	--

Table 2.9 Comparison of the different silica sources available for the synthesis of silica-based mesoporous materials.

Development of ordered mesoporous silica materials is tightly related to the development of the sol–gel process. Historically, sol–gel technology to form silica originates from the hydrolysis of tetraalkoxysilanes ($\text{Si}(\text{OR})_4$) in the presence of either acid or basic catalysts. Mesoporous silica materials are typically synthesized by using tetraethoxysilane ($\text{Si}(\text{OCH}_2\text{CH}_3)_4$), TEOS and TMOS ($\text{Si}(\text{OCH}_3)_4$). Because of its lower price and lower toxicity, TEOS is much more often used than TMOS. Indeed, methanol vapours released as a by-product of TMOS hydrolysis are known to be toxic to eyes and can cause blindness. Successful use of TEOS in the synthesis of organized mesoporous silica is due to the possibility of tailoring the silicate oligomers present in solution by regulating the experimental conditions of hydrolysis and condensation (118-120). Structures and different degrees of polymerization of the polysilicic acids can indeed affect their ability to interact with the organic templates through electrostatic interaction or hydrogen bond formation. Major drawbacks of silicon alkoxides are their toxicity and high cost that limit their development from the laboratory to the industrial scale (121).

In the case of more sustainable production of silica mesostructures, soluble silicates have recently attracted much attention owing to their low price and low toxicity compared to silicon alkoxides. Soluble silicates are purely inorganic amorphous glasses and are mainly used in the form of aqueous alkaline sodium silicate solution (Na_2SiO_3 , also known as water glass or liquid glass), fumed silica and colloidal silica. Soluble silicates have been successfully used in chemical grouting and other geotechnical applications (122). They are also used as detergents and flocculating agents. Sodium silicate solutions, colloidal silica and fumed silica are the most used inorganic silica sources for the preparation of organized mesoporous silica. The low cost of these inorganic precursors is due to their methods of production that involve the direct transformation of natural quartz deposits. Regarding the large variety of the silica

mesostructures generated, differences between silicon alkoxides and soluble silicate precursors are not so obvious (123).

A natural silica source is defined as a non-toxic silica-containing mineral that is extracted from natural deposits and that can be straightaway used as a reagent in the synthesis of mesoporous silica. Synthesis procedures starting from natural silica sources involved a first step of pre-treatment under acidic or basic conditions and at mild temperatures to extract silicate species from the material. But in contrast to synthetic silica sources (TEOS, water glass, colloidal silica, fumed silica, etc.), both chemical composition and structure of the natural silica source are very close to that of the corresponding raw material. The exploitation of these silica sources does not imply any energy intensive and non-ecological silicon extraction or chemical transformation steps and therefore they can be considered as readily available chemical sources (124, 125).

Recycled industrial and agricultural by-products that contain silica were recently considered as abundant silica resources. In addition to converting toxic wastes into high value silica-based materials, recycling processes afford solutions to solve the problem of waste disposal and to guarantee the long-term availability of natural silicon resources (126).

2.7.2 Functionalization of MSNs

Two different pathways are available to functionalize the synthesized mesoporous silica nanoparticles (127):

- 1) The subsequent modification of the pore surface of a purely inorganic silica material (“grafting”).
- 2) The simultaneous condensation of corresponding silica and organosilica precursors (“cocondensation”).

2.7.2.1 Post synthetic functionalization of silicas (“Grafting”)

Grafting refers to the subsequent modification of the inner surfaces of mesostructured silica phases with organic groups. This process is carried out primarily by reaction of organosilanes of the type $(R'O)_3SiR$, or less frequently chlorosilanes $ClSiR_3$ or siloxanes $HN(SiR_3)_3$, with the free silanol groups of the pore surfaces (Figure 2.10). In principle, functionalization with a variety of organic groups can be realized in this way by variation of the organic residue R.

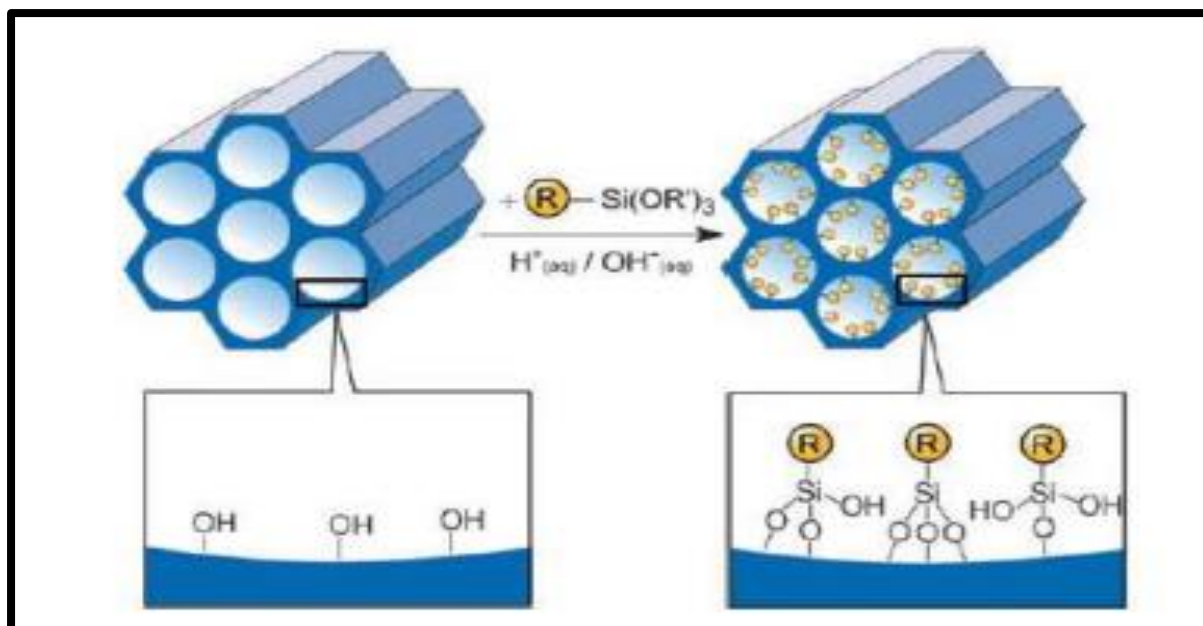


Figure 2.10: Grafting (post synthetic functionalization) for organic modification of mesoporous silica with terminal organosilanes of the type $(R'O)_3SiR$. R=organic functional group.

This method of modification has the advantage that, under the synthetic conditions used, the mesostructures of the starting silica phase is usually retained, whereas the lining of the walls is accompanied by a reduction in the porosity of the hybrid material (albeit depending upon the size of the organic residue and the degree of occupation). If the organosilanes react preferentially at the pore openings during the initial stages of the synthetic process, the diffusion of further molecules into the center of the pores can be impaired, which can in turn lead to a nonhomogeneous distribution of the organic groups within the pores and a lower degree of occupation (128-130). In extreme cases (e.g., with very bulky grafting species), this can lead to complete closure of the pores (pore blocking).

2.7.2.2 Co-Condensation (Direct synthesis)

An alternative method to synthesize organically functionalized mesoporous silica phases is the co-condensation method (one-pot synthesis). It is possible to prepare mesostructured silica phases by the co-condensation of tetraalkoxysilanes $[(RO)_4Si]$ (TEOS or TMOS) with terminal trialkoxyorganosilanes of the type $(R'O)_3SiR$ in the presence of structure-directing agents leading to materials with organic residues anchored covalently to the pore walls (Figure 2.11). By using structure-directing agents known from the synthesis of pure mesoporous silica phases

(e.g., MCM or SBA silica phases), organically modified silicas can be prepared in such a way that the organic functionalities project into the pores.

Since the organic functionalities are direct components of the silica matrix, pore blocking is not a problem in the cocondensation method (131). Furthermore, the organic units are generally more homogeneously distributed than in materials synthesized with the grafting process. However, the cocondensation method also has several disadvantages: in general, the degree of mesoscopic order of the products decreases with increasing concentration of $(R'O)_3SiR$ in the reaction mixture, which ultimately leads to totally disordered products (132). Consequently, the content of organic functionalities in the modified silica phases does not normally exceed 40 mol%. Furthermore, the proportion of terminal organic groups that are incorporated into the pore-wall network is generally lower than would correspond to the starting concentration of the reaction mixture (133).

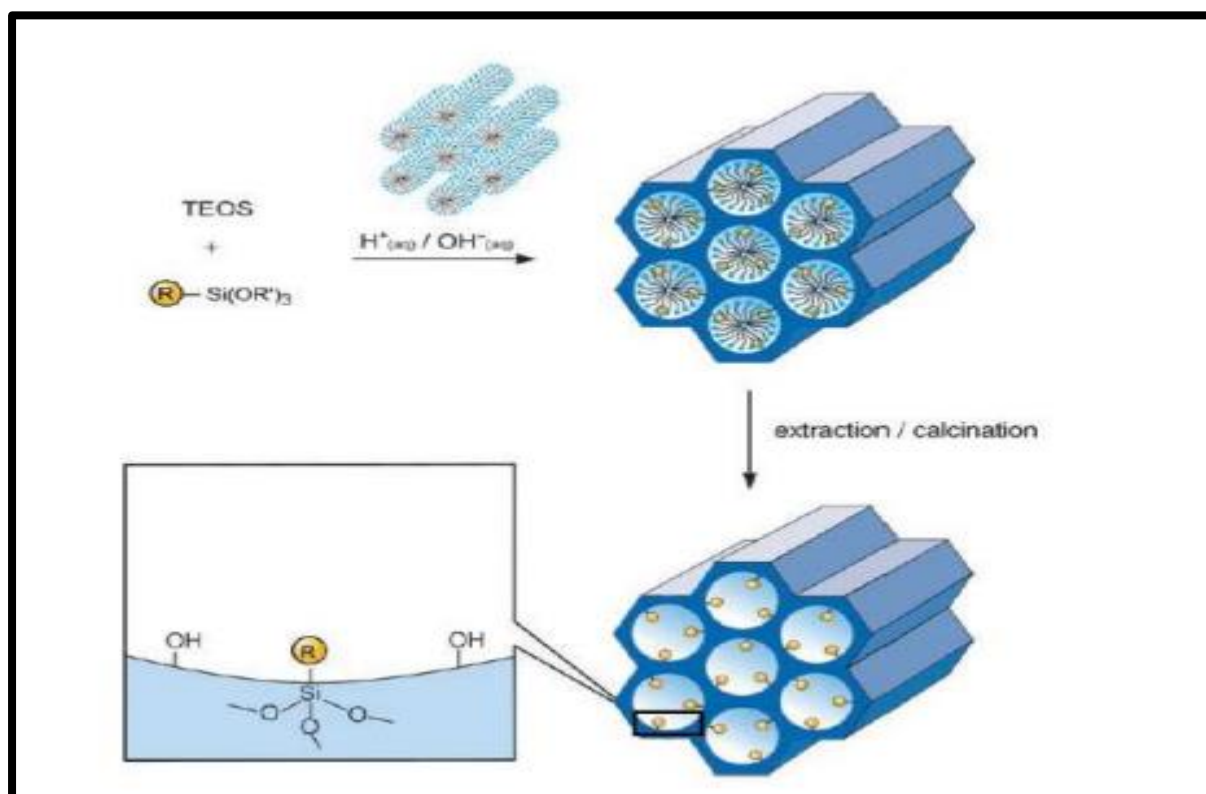


Figure 2.11: Co-condensation method (direct synthesis) for the organic modification of mesoporous silica. R=organic functional group.

2.8 Mesoporous Silica based drug delivery systems (DDS) for cancer therapy

With the versatile and tunable structures, MSNs have been proven to be capable of loading a variety of guest molecules including pharmaceutical drugs, therapeutic peptides and proteins

and genes. MSNs have been used as drug delivery systems of kinds of chemotherapeutic drugs of different hydrophobic/hydrophilic properties, molecule weights, and biomedical effects such as doxorubicin, camptothecin, cisplatin, paclitaxel, docetaxel, methotrexate etc (134).

2.8.1 Active targeting of cancer cells by MSNs based drug delivery systems (DDS)

Active targeting as a complementary strategy to EPR effect has opened a new area for traditional chemotherapy to enhance the efficiency of anti-cancer, which known as ligand-mediated targeting involving functionalization of the MSNs surface with active targeting ligands. The active targeting ligands, such as small molecules, peptides, antibodies, proteins, saccharides, and aptamers, have specific affinity to the over-expressed receptors on the tumor cells. Typically, there are three paths (targeting to tumor vessels, tumor cells, nuclear) to achieve effective enrichment of drugs in tumor tissues. The most relevant results derived from the conjugation of active targeting ligands to MSNs-based nanosystems to promote specific recognition and cellular uptake by cancer cells are summarized in Table 2.10

Site	Targeting ligand	Targets/ mechanism	Model	Model drug	Ref
Tumor cell membrane	Hyaluronic acid (HA)	CD44 receptor	MDA MB 231	Rhodamine B	(135)
	Hyaluronic acid (HA)	CD44 receptor	HCT-116	Doxorubicin	(136)
	Folic acid (FA)	Folate receptor	A549, HeLa	Doxorubicin	(137)
	Anti EpCAMDNA aptamer (AP)	EpCAM	SW620	Doxorubicin	(138)
	YY146 (an anti-CD146 antibody)	CD 146	U87MG	Doxorubicin	(139)
	Antibody/single-chain variable fragment (Ab-scFv)	Specific receptor affinity	OVCAR – 5	Bevacizumab	(140)
	K4YRGD peptide	$\alpha\beta$ 3 receptor	HepG2	Doxorubicin	(141)
	Lactose	ASGPR	HepG2	Docetaxel	(142)
	AS1411 aptamer	Nucleolin	HeLa	Docetaxel	(143)

	N3GPLGRGRGDK- Ad	$\alpha\beta$ 3 integrins	SCC – 7	Doxorubicin	(144)
	PEI – cRGD	$\alpha\beta$ 3 integrins	Blood brain barrier	Doxorubicin	(145)
	cRGDfK	$\alpha\beta$ 3 integrins	MDA MB 231 triple negative breast cancer	Arsenic trioxide (As ₂ O ₃)	(146)
	CRGDKGPDC	α 2 β 3 receptor	HeLa	Combretastatin and Doxorubicin	(147)
	CRGDyK	$\alpha\beta$ 3 integrins	U87MG	Sunitinib (SUN)	(148)
	HB5 aptamer	HER2	SK-BR-3	Doxorubicin	(149)
	Anti TRC 105	CD105	HUVE-Cs	Doxorubicin	(150)
Nuclei	TAT peptide	Nuclear membrane receptors	MCF – 7 ADRs	Doxorubicin	(151)
	MONs-PTAT	Nuclear membrane receptors	HeLa	DNA	(152)
	MSN-TAT-K ₁₁	Stepwise acid active	HeLa	Doxorubicin	(153)
	Dexamethasone (DEX)	Glucocorticoid receptor	HeLa	Doxorubicin	(154)
Multistage target Tumor and nuclei	FA and Dexamethasone (DMX)	Folate receptor and Glucocorticoid receptor (GR)	HeLa	Doxorubicin	(155)

Tumor cell and vessels	tLyp-1-peptide	Neuropilin (NRP)	MDA MB 231, HUVECs	Doxorubicin	(156)
------------------------	----------------	------------------	--------------------	-------------	-------

Table 2.10: Active targeting ligands conjugated to mesoporous silica nanoparticles-based nanosystems that permit their specific recognition.

Different from normal tissues, many proteins show specific over-expression on the surface of tumor-associated endothelial cells due to the abnormal overgrowth of intratumoral vasculature, which can be utilized as targets for targeted drug delivery and cancer treatment. According to the literature, targeting to the endothelial cells of the tumor vessels and subsequently killing them can lead to the necrosis of tumors because tumor vasculatures are the transport channel of nutrition which guarantees the fast proliferation of tumor cells, which has become a promising alternative in treating solid tumors. In 2013, Chen *et al.*, reported the first example of in vivo tumor vascular targeted drug delivery system based on MSNs. In this nanosystems, TRC105 antibody targeting to CD105 receptor was conjugated onto MSNs surface. In the 4T1 tumor tissue, the receptors (CD105) only overexpressed in the tumor vasculature but did not express on 4T1 tumor cell. Various tumor vascular targeting ligands, such as vascular endothelial growth factor (VEGF) specific for VEGF receptors (VEGFRs), arginine-glycine-aspartic acid (RGD) peptides targeting to $\alpha v \beta 3$ integrin receptor, HB5 aptamer which was specific for human epithelial growth factor receptor 2 (HER2), anti-VCAM-1 monoclonal antibody specific for vascular cell adhesion molecule-1 (VCAM-1) receptors, have been connected to the surface of MSNs to develop vascular targeted drug delivery systems with enhanced therapeutic efficiency. Very recently, Li *et al.* reported a novel vascular-targeting co-delivery DDS based on targeting molecules (iRGD peptide) modified MSNs. In this system, antiangiogenic agent (combretastatin A4) and chemotherapeutic drug (DOX) were payloaded, leading to significantly improved anti-cancer efficacy even at a very low DOX dose (1.5mg/kg). Furthermore, the disruption of vascular structure caused by combretastatin A4 which was released quickly at tumor vasculatures had a synergetic effect with DOX which released slowly in the subsequent delivery of DOX into tumors.

After reaching tumor tissues, drug loaded nanocarriers are often expected to target to tumor cells through specific interaction between ligand and receptor, leading to the enhanced cellular uptake and drug delivery efficiency and the enhanced therapeutic efficacy. Ligand mediated targeting to tumor cells need meet the following requirements: (I) A threefold overexpression of the targeted receptor on the cancer cell compared with normal cells is generally considered

to be sufficient to warrant further investigation, although greater upregulation is preferred. (II) The density of active targeting ligands on the surface of nanoparticles should be carefully manipulated and optimized to obtain maximized targeting and therapy efficiency. Because the ligand/ nanoparticle ratio strongly affects the cell recognition specificity, so greater selectivity and targeting efficiency can be obtained with higher density of active targeting ligands. But excessively high density of active targeting ligands may increase the steric hindrance effect and lead to poor cellular uptake efficiency. (III) Preventing targeting ligands coated by the plasma protein is also a noteworthy issue because the targeting ligands can be shielded by opsonization, which can result in loss of their targeting ability in a complex in vivo environment. (IV) The targeted receptor on the cancer cell can induce endocytosis. Various tumor cell targeting ligands such as antibodies (anti-CD146 antibody, antibody fragment (Ab/scFv)), proteins (transferrin (Tf)), peptides (K4YRGD peptide), saccharides (hyaluronic acid (HA), lactobionic acid (LA), Lactose, small molecules (folic acid (FA), aptamers (anti-EpCAMDNA aptamer, AS1411 aptamer), have been conjugated onto MSNs surface to receive tumor cell targeted property. y. Quan *et al.* designed a hepatoma targeting DDS based on lactose conjugated MSNs (Lac-MSNs) with anticancer drug DTX loaded. The DTX-Lac-MSNs showed specific targeting to ASGPR positive SMMC7721 and HepG2 cells, and the cellular uptake of Lac-MSNs was an energy consuming process and predominated by clathrin-mediated endocytosis. Thanks to active targeting, significantly enhanced inhibition of the growth of HepG2 and SMMC7721 cells in vitro was obtained.

2.8.2 Stimuli responsive Mesoporous Silica Nanoparticles (MSNs)

The value of having the most selective targeting system is of course lost if the cargo is released from the carrier before it reaches the target site. For chemotherapy applications it is desirable that no release of cargo should occur in the extracellular environment, while a fast release of the cargo should occur once the carrier particle has reached its point of action. The release of cargo from mesoporous silica is often diffusion-controlled and typically associated with a pronounced initial burst. Therefore, there is a strong current interest in the development of means to prevent a fast initial release of the cargo, which in the optimal case would be sensitive to the local environment of the carrier particles in a way that release of the cargo is only triggered inside the cells or within specific cellular compartments after internalization.

Stimuli-responsive MSNs only release the cargos in the targeted cancer sites upon triggering by intratumoral stimuli (pH, redox, enzyme, temperature) or exogenous stimuli (magnetic field,

ultrasound, light) with nearly no premature drug release. Stimuli-responsive MSNs have been regarded as promising approach to improve the therapeutic effect of anticancer agent and simultaneously reduce the undesirable side effects to normal cells.

2.8.2.1 Internal stimuli-responsive MSNs

Various kinds of tumor tissues share similar microenvironment distinct from normal ones, such as leaky vasculatures, acidic and hypoxic environments, high redox potential, increased level of cancer-associated enzymes and higher local temperature. Based on these, stimuli-sensitive delivery system can be designed to response to the tumor (157).

2.8.2.2 pH responsive MSNs

Among the various stimuli-sensitive DDSs, pH-responsive CDDSs have been widely researched since the human body exhibits variations in pH (158). The pH value approximately 7.4 in extracellular of normal tissues and blood, while between 6.0 and 7.0 in tumor microenvironment, which is mainly caused by high level of CO₂ and high glycolysis rate. The pH value will decrease further inside cancer cell such as endosomes (pH=5.5-6.0) and lysosomes (pH=4.5-5.0). The pH-responsive nanosystems based on MSNs are shown in Table 2.13.

Type	Material	pH-responsive mechanism
Acid cleavable linker/bond	gold NP-acetal linker- MS	Acetal linker
	lanthanide doped NP-acetal bond-MS	Acetal bond
	Fe ₃ O ₄ NP- boronate ester bond-MSN	Boronate ester bond
	Poly(N-succinimidyl acrylate)-acetal linker-MS	Acetal linker
	MSN-hydrazone-Dox	Hydrazine
	Dox@PAA-ACL-MSN	ACL
	Au NPs-DNA-MSNs	DNA
Polymer gatekeepers	Dox-MSN s-Gelatin	Gelatin
	Dox-MSNs-chitosan	Chitosan
	Dox@MSNs-PVP-PEG	PVP
	DOX@MSNs-PLGA	PLGA

	PAH /PSS MSNs	PAH/PSS polyelectrolyte multilayers
	Alginate/Chitosan-NH ₂ -MSNs	Alginate/Chitosan Multilayers
	Chitosan /dialdehyde starch-MSNs	chitosan/dialdehyde starch polyelectrolyte multilayers charge-reversal
	PAH-cit/APTES-MSNs	polymer PAH-cit
	Cur@PAMAM- MSNs	PAMAM
	PDEAEMA- MSNs	PDEAEMA
	Dox@PAA-MSNs	PAA
	Dox@PEMA/PEG-MSNs	PEMA
	i-motif DNA-MSNs	i-motif DNA
Supramolecular nanovalves	β - cyclodextrin caps- aromatic amines stalks-MSNS	Aromatic amines stalks
	α -cyclodextrin- p-anisidino stalks - MCM-41	p-anisidino stalks
	cucurbit(6)uril-trisammonium stalks MSNs	Trisammonium stalks
Acid decomposable gatekeepers	ZnO@MSN	ZnO
	Dox-Si-MP-CaP	pH-Tunable calcium phosphate
	LDHs-MSNs	LDHs

Table 2.13 The pH responsive nanosystems based on MSNs

PAA, Polyacrylic acid; ACL, acid cleavable linker; PVP, polyvinylpyrrolidone; PEG, poly(ethylene glycol); PLGA, poly(lactic-co-glycolic acid); PAH, poly(allylamine hydrochloride); PSS, poly(styrene sulfonate); PAMAM, (polyamidoamine); PDEAEMA, Poly(2- (diethylamino)ethyl-methacrylate); PPEMA, poly(2-(pentamethyleneimino)ethyl-methacrylate); CaP, calcium phosphate; LDH, layered double hydroxides.

The pH-sensitive linkers, such as acetal bond, hydrazine bond, hydrazone bond and ester bond can be cleaved under acidic condition, thus providing opportunities for designing pH-responsive DDS applied in cancer treatment (158). Liu et al reported a new pH-responsive

nanocarrier by capping gold nanoparticles onto the surface of mesoporous silica through acid-labile acetal linkers. [Ru(bipy)₃]Cl₂ dye was loaded as a model drug to investigate the pH-responsive release behaviour, and the dye-loaded MSN was dispersed in water at different pH values to test the release profiles. At pH 7.0, no free dye was observed as the intact acetal linker and gold nanoparticles blocked the nanopores to inhibit cargo release. However, the solution at pH 4.0 induced a quick release of dye molecules and almost 100% dye molecules were totally released in 13 hours. On decreasing the pH to 2.0, an even faster molecular transport was observed with 90% release within 30 minutes and reached equilibrium in 2 hours. Similarly, a pH-responsive nanocarrier was designed by Chen et al via capping graphene quantum dot (GQD) onto the nanopores of mesoporous silica through an acid-cleavable acetal bond. The amount of drug leaked from GQD@MSN remained negligible (nearly 3.5%) after 24 hours of incubation, indicating that GQD caps can efficiently block the nanopores. However, ~48% and 86% of the drug molecule were released when the pH value decreased to 5.0 and 4.0, respectively. The accelerated DOX release was ascribed to the cleavage of the acetal bond under the acidic conditions and the continuous separation of GQDs from MSN. Besides that, hydrazine bond is another widely studied acid-labile linker.

Polyelectrolyte is a commonly used blocking material in pH-responsive drug delivery. Feng et al constructed an MSN-based pH-responsive DDS with polyelectrolyte multilayers. Polyallylamine hydrochloride and polystyrene sulfonate were coated onto the surface of MSN via a layer-by-layer technique, and doxorubicin hydrochloride (DOX) was loaded into the nanopores of the as-prepared polyelectrolyte multilayer (PEM)-MSN(159). Results showed that there was a tendency of layer thickness-dependent drug release, and MSN with 20 layers exhibited the highest DOX release rate. Moreover, MSN at acidic condition (pH 5.2) showed a significant higher drug release rate than those at neutral condition (pH 7.4).

2.8.2.3 Redox responsive MSNs

The development of redox-responsive vehicles for targeted intracellular drug/gene delivery is a very efficient cancer therapeutic strategy. The basic principle of redox-responsive DDS is based on the significant differences in redox concentrations between tumors and normal tissues. It is well documented that concentration of reducing agents such as glutathione (GSH) existing in tumor cells is approximately three times higher than that in normal cells. As a redox-sensitive group, the disulphide bond (S–S) could be easily cleaved in the presence of GSH, which makes it an attracting receptor site in the design of redox-responsive DDS. Many inorganic

nanoparticles have been used as nanovalves to seal the drug molecule into the channels of MSN through covalently functionalizing MSN with disulphide containing linkers, such as CdS, Fe₃O₄, gold and ZnO.

Type	Material	Mechanism
Redox responsive	CdS, Au, Fe ₃ O ₄	Inorganic NPs- disulphide bonds-MSNs
	poly(propyleneimine) dendrimers, PEG, heparin, peptides, polyethyleneimine(PEI), cyclodextrin, PDS, cytochrome c, PEG-PCL	Organic molecules disulphide bonds-MSNs
	mPEG@6-MP@CMS HA@6-MP@CMS	Thiolated drug-disulphide bonds-MSNs
	MSN@MnO ₂	Glutathione degradable gatekeepers

Table 2.14 Redox-responsive nanosystems based on MSNs

Zhang et al reported redox-responsive nano-gated MSN by grafting β -CD or adamantane onto the nanopores of MSN through disulphide. After the drug-loaded nanoparticles internalized and then escaped from the endosome to diffuse into the cytoplasm of cancer cells, the high concentration of GSH in the cytoplasm leads to the removal of the β -CD/adamantane caps by cleaving the pre-installed disulphide bonds, further promoting the release of drugs from the nanocarriers.

2.8.2.4 Enzyme responsive MSNs

The upregulated expression profile of specific enzymes in pathological conditions such as cancer makes it an interesting stimulus to achieve enzyme-mediated drug release. Recently, the developments of enzyme-triggered DDS based on functionalized MSN have attracted much attention. As one of the important physiological changes in the tumor microenvironment, matrix metalloproteinases (MMPs), especially MMP2 and MMP9, are overexpressed in almost all the types of cancer cells and associated with tumor invasiveness, metastasis, and angiogenesis, whereas they are minimally expressed in healthy tissues.

Type	Material	Mechanism
Enzyme responsive	MSN-GFLGR7-RGDS/ α -CD	Protease-sensitive crosslinker
	DNA68 HA69 gelation, cellulose, galacto-oligosaccharide	Enzyme degradable polymer

Table 2.12 Enzyme-responsive nanosystems based on MSNs

Recently, specific protease-sensitive peptide sequences have been designed as linkers that allow the controlled release of chemotherapeutics from MSN. Rijt et al developed avidin-capped MSN functionalized with linkers that could be specifically cleaved by MMP9, thereby allowing controlled release of chemotherapeutics from MSN in high MMP9-expressing lung tumor cells. The avidin-capped MSN demonstrated an efficient protease sequence-specific release of the incorporated chemotherapeutic cisplatin and a rapid tumor cell apoptosis.

2.8.2.5 Temperature responsive MSNs

Thermo-responsive drug delivery is one the most investigated stimuli-responsive strategies and has been widely explored in tumor therapy. Thermo-responsive MSN DDSs are usually composed of MSN and surface-coated thermo-responsive materials. The drug release was closely dependent on the variation of the surrounding temperature to control the switch of the nanovalves. Poly N-isopropyl acrylamide (PNIPAM) has been well known as a thermo-responsive polymer.

Type	Material	Mechanism
Thermo-responsive	poly(ethyleneoxide-b-N-vinylcaprolactam), Zwitterionic sulfobetaine copolymers, paraffins supramolecules, rotaxane, copolymer-lipid bilayers	Thermo-sensitive polymerization
	DNA, peptide sequences	Thermo sensitive bio-molecules

Table 2.13 Thermo-responsive nanosystems based on MSNs

2.8.2.6 External stimuli sensitive MSNs

Unlike endogenous stimuli, exogenous stimuli are carried out via an external physical treatment. Although this approach seems unappealing, exogenous stimuli-responsive DDSs might be more encouraging and favourable due to the heterogeneous physiological conditions

of human population. Various externally applied stimuli include magnetic fields, ultrasounds, and light.

2.8.2.7 Magnetic responsive MSNs

Magnetic-responsive DDS relies on the delivery of magnetic and drug-loaded nanoparticles to the tumor site under the influence of external magnetic field. The external magnetic field can not only drive the magnetic nanoparticles to the desired location precisely, but also can act as an exogenous stimulus to induce the controlled drug release. Superparamagnetic iron oxide nanoparticle is one of the most widely employed magnetic particles.

Type	Material	Mechanism
Magnetic responsive	Poly(N-isopropylacrylamide/N hydroxymethylacrylamide), poly(ethyleneimine)-b-poly(N isopropylacrylamide), lipid bilayer, pseudo rotaxanes	Heat produced by AFM + thermo-sensitive gatekeeper
	mNPs+DNA+MSNs Azo-PEG@ Fe ₃ O ₄ @SiO ₂	Heat produced by AFM + thermally unstable chemical linkers
	SPION@MSN-DA	Heat produced by AFM + thermally reversible cycloreversion reaction

Table 2.14 Magnetic responsive nanosystems based on MSNs

2.8.2.8 Ultrasound (US) responsive MSNs

Ultrasound is one of the most promising exogenous stimuli for drug delivery with the advantages of non-invasiveness, ability of deep tissue penetration, and controllable frequency. Moreover, ultrasonic irradiation could enhance drug release rate from both biodegradable and non-biodegradable polymer matrices.

Type	Material	Mechanism
Ultrasound responsive	MSNC@Au-PFH-PEG	Ultrasound sensitive material cavitation
	p(MEO2MA)-co THPMA	Ultrasound- cleavable moieties

	Fc-CONH-MS	Ultrasound sensitive of ferrocene derivative
--	------------	--

Table 2.15 Ultrasound (US) responsive nanosystems based on MSNs

2.8.2.9 Light responsive MSNs

Due to their non-invasiveness property and the possibility of remote spatiotemporal control, a variety of light-responsive systems have been developed in recent years to achieve on-demand drug release in response to light irradiation at a specific wavelength (in the ultraviolet [UV], visible, or near-infrared regions). The mechanism relies on the photo-sensitiveness-induced conformational transition of the nano-carriers.

Azobenzene (AB) is a type of light-sensitive molecule. When irradiated with UV light at a wavelength of 351 nm, AB can isomerize from the more-stable trans to a less-stable cis configuration. Different studies have demonstrated that there was a high binding affinity between β -CD and trans-AB derivatives and a low binding affinity between β -CD and cis-AB derivatives in aqueous solutions. According to this principle, a lot of AB-labile light-responsive DDSs were designed.

Type	Material	Mechanism
UV-Vis light responsive	β -CD and/ or Py- β -CD- azobenzene stalks-MSNs α -CD-azobenzene stalks-MSNs	The isomerized of azobenzene group from cis to trans
	thymine derivatives-MSNs o-nitrobenzyl ester moiety -MSNs poly(N-isopropylacrylamide-co-2-nitrobenzylacrylate)-MSNs	Photo responsive polymers gatekeeper
	7-amino-coumarin derivative (CD)-MSNs, S-coordinated Ru(bpy) ₂ (PPh ₃)- moieties-MSNs, TUNA-MSNs	Photo responsive linkers
NIR light responsive	DNA-Au@MSNs DNA-Cu _{1.8} S@mSiO ₂	NIR-absorbing materials, thermal-responsive material

	1-tetradecanol-GNR@MSNs sulfonatocalix[4]arene- AuNR@MSN Au-nanocage@mSiO ₂ @ PNIPAM CuS@mSiO ₂ -PEG SWNT@MS-PEG UCNP@mSiO ₂ -Ru	
--	---	--

Table 2.16 Light responsive nanosystems based on MSNs

2.8.2.10 Multi stimuli responsive MSNs

Compared to single stimuli-responsive drug delivery systems, dual or multi-responsive DDSs are sensitive to two or more stimuli, either in a synergistic fashion or in an independent style, which has gained considerable attention in the current decades for its capability of further improving the delivery. Table 2.17 represent the different multi stimuli responsive approached developed using mesoporous silica as a carrier.

Mechanism	Material	Release condition	Biological model	Model drug
pH/ cellulose/redox/enzyme	Cellulose HA	pH 4.0/ cellulose GSH/ hyaluronidases	HepG2 HCT – 116	DOX DOX
pH/redox/UV	PDEAEMA/disulphide bond/o-nitrobenzyl ester	pH 5.0/ DTT/UV	HeLa	DOX
NIR/pH/thermo	Au25(SR)18/P(NIPAm- MAA)	980nm(NIR)/ tumor sites	A549, HeLa, SKOV3	DOX
pH/redox	poly(allylamine hydrochloride) citraconic anhydride/galactose- modified trimethyl chitosan-cysteine	pH5.0/ Cytoplasmic glutathione	QGY- 7703	DOX/ siRNA

Esterase/pH	poly(β -amino ester)	liver esterase/pH <5.0	MDA- MB-231	DOX
Enzyme/Redox or thermo/Redox/pH enzyme	AND logic gates(DNA) AND logic gate (PAA/PCL)	DNase I/DTT or 50°C/DTT pH5.5@esterase	A549 SK- N-BE(2), HeLa, MRC-5	Calcein DOX
pH/redox	Disulphide bonds/ benzoic-imine bond	Glutathione/ pH5.0	U87MG	DOX
Magnetic/NIR	Fe ₃ O ₄ @poly-L- lysine@ Au@ dsDNA	Magnetic Target/ 808nm NIR	HeLa, nude mice	DOX
Ultrasound/pH/ Magnetic	Crown-Ether/SPION	Ultrasound/pH/ Magnetic	L929	DOX

Table 2.17 Multi stimuli responsive nanosystems based on MSNs

Very recently, Zhang et al. reported a reduction, pH, and light triple responsive nanocarriers (HMSNs-PDEAEMA) based on hollow mesoporous silica nanoparticles (HMSNs) coated by poly (2-(diethylamino)-ethyl methacrylate) (PDEAEMA). pH-sensitive PDEAEMA polymer capped on the surface of HMSNs through linkages including reduction cleavable disulphide bond and light-cleavable o-nitrobenzyl ester. DOX was easily loaded into the nanocarriers with high drug loading efficiency, and the rapidly released of DOX was triggered by the stimuli of acid environment, reducing agent or UV light irradiation. In addition, the results of flow cytometry analysis, CLSM and cytotoxicity indicated that the DOX loaded HSNs-PDEAEMA was efficiently uptake by HeLa cells, showing (i) smart control on drug delivery and release, (ii) the enhanced DOX release into the cytoplasm under external UV light irradiation, and (iii) higher cytotoxicity against HeLa cells.

2.8.3 Multi-functional MSNs for theranostic applications

Theranostic nanomedicines combine the therapeutic and diagnostic agents on a single platform to simultaneously monitor and treat the disease. Besides the therapeutic agent, the theranostic nanoparticles should contain contrast agents or molecular probes to characterize biological processes at the cellular and subcellular levels for diagnostic purposes, using optical imaging, computed tomography (CT), radionuclide imaging, and magnetic resonance imaging. Among

other theranostic nanomedicines, MSNs have attracted an increased interest for theranostic purposes, mainly due to their ability to carry different cargoes simultaneously and their intrinsic optical and photochemical properties.

Yang et al. prepared magnetic MSNs (M-MSNs), with the core consisting of Fe₃O₄-Au NP and photosensitizer Ce6 and DOX adsorbed onto their surface. Next, polyelectrolyte multilayers (PEM) composed of biocompatible alginate/chitosan were assembled on the M-MSNs to fabricate a pH-responsive drug delivery system and adsorb P-gp shRNA (MMSN(DOX/Ce6)/PEM/P-gp shRNA nanocomposite) to overcome the multidrug resistance. The *in vivo* therapeutic efficacy of final M-MSN(DOX/Ce6)/PEM/P-gp shRNA nanocomposites (average diameter 280 nm) was compared with the respective controls using EMT-6 tumor bearing Balb/c female mice, with initial tumor size of 0.8–1.6 cm³. The group treated with M-MSN(DOX/Ce6)/PEM/P-gp shRNA nanocomposite with laser irradiation accomplished a significant tumor ablation because of the combined chemotherapy, PDT, and gene therapy of cancer *in vivo*. Moreover, the measured body weight of mice during the treatment showed no significant changes, suggesting that the treatment with the nanocomposite was not severely toxic within the 18 d of treatment. Therefore, the developed multifunctional nanocomposites were able to be used as an efficient nanoprobe for magnetic resonance and X-ray CT imaging of both *in vitro* and *in vivo* xenografted tumor models.

2.8.4 Biodegradation and clearance of MSNs

MSN biodegradation and clearance are strongly interdependent processes. MSNs dissolve rapidly under physiological conditions when the concentration levels are kept below the saturation level of silica, as demonstrated in several *in vitro* studies. The rate of silica dissolution is dependent on parameters such as the particle size, functionalization, and the degree of silica condensation, which in turn is highly dependent on the heat-treatment history of the silica particles. For circulating particles, the liquid (aqueous) volume is typically large with respect to the silica concentration and, therefore, it can be expected that the particles dissolve under *in vivo* conditions. Dissolved silica is known to be adsorbed by the body or excreted in urine in the form of silicic acid or oligomeric silica species. Here, forces exerted by blood pressure would be expected to assist in disintegration of partially dissolved particles, which can be expected to have a lower mechanical stability as compared with the original particles. Interestingly, it has been observed that, depending on the particle size, the particles can dissolve from inside out leaving the initial particle size virtually intact under static conditions. This has

also been corroborated by recent *in vivo* data, where partially degraded MSNs with particle dimensions close to that of the injected particles were found in urine, suggesting the same degradation mechanisms may also be operative *in vivo*. However, the renal cut-off limit is approximately 5 nm, which is why the exact excretion process remains unclear in this case. Landry and co-workers investigated rat urine after intraperitoneal injection of tetra ethylene glycol functionalized Gd-containing mesoporous microparticles and found particle-shaped objects most likely originating from the microparticles and concluded that particulates could also be partially excreted renally. This observation was also corroborated by MRIs of the lower abdominal cavity of the Wistar rats used, demonstrating enhanced contrast in the bladder at time points 2–25 h post injection. As the animals did not exhibit any signs of Gd³⁺ toxicity up to 1-week post injection, the signal was not likely to be caused by free Gd³⁺. Huang et al. found the same phenomenon for their studied MSN rods, when they were able to image (by TEM combined with energy dispersive x-ray spectroscopy) MSNs in both urine and faecal samples at 24 h post administration (*iv.*) confirming by energy dispersive x-ray spectroscopy that they consisted of silica elements. Also, Lu et al. were able to TEM-image intact MSNs in urine samples. In the *iv.* biodistribution study by He et al., they found distinctly less degradation products in the urine at shorter time points (30 min) for PEGylated MSNs than for non-PEGylated MSNs; and the degradation products also increased with increasing particle size. They concluded that this observation was because MSNs of larger particle sizes were more easily captured by the liver and spleen in 30 min, which led to their faster biodegradation and thus larger excreted quantities of their degradation products, whereas the PEGylation would hinder the capture by these RES organs and consequently slow down the biodegradation. The biodegradation and elimination mechanisms based on this argumentation, however, remain unclear. Also, the urine analysis relied on absolute fluorescence (FITC) values, which suggests the results should be interpreted as indicative. However, when combined with ICP analyses, Lu et al were able to correlate the fluorescence observed in a smear of urine at 4 h post injection (*iv.*) to that of the amount of Si in the urine, for which the highest amount was detected 24 h post injection. By contrast, the excreted amount of Si in faeces increased with time and peaked at the last time point (4 days), at which nearly all Si injected was excreted. It is important to note that no background level was recorded. The authors pointed out that the silica content in the faeces was very small compared with that of urine. On this topic, Lo and coworkers²⁶¹ studied the effect of the surface charge on the two proposed elimination routes of MSNs and found that MSNs with high positive charge exhibited rapid hepatobiliary excretion. They found correlations between fluorescence and ICP analyses, but in this case both the negatively and

positively charged MSNs (size 50–100 nm) entered hepatobiliary transport within 24 h of injection, with no detectable renal excretion. In this case, the background Si levels (dietary sources) were determined, which otherwise often seems to be overlooked in ICP analyses of urine and organs, and thus they could pinpoint the peak excretion to occur 2 days postinjection. However, based on organs harvested and ICP-analysed 3 days postinjection, it was suggested that a possible onset of MSN biodegradation to orthosilicic acid with potential renal excretion could be operative. For the differently charged particles studied, they concluded that while both were sequestered by the liver; the one with the higher charge could have been more opsonized by serum proteins and thus more amenable to hepatobiliary excretion into the GI tract. Thus, surface charge tuning could not only constitute a complement for targeting but also a means for regulation of the rate of excretion.

2.8.5 Safety and toxicity of MSNs

The number of studies regarding safety and toxicity of MSNs has increased rapidly during the last years. In a recently published study MSNs showed significantly less cytotoxicity and apoptotic cell death and lower expression of proinflammatory cytokines than colloidal silica nanoparticles *in vitro*, and MSNs neither induced contact hypersensitivity nor acted as immunogenic sensitizer *in vivo*, which was shown with local lymph node assay. Depending on the type of MSNs studied to date, quite different conclusions have been drawn. On a very general level, surface functionalized MSNs seem to reduce the observed harmful effects as compared with pristine mesoporous silica. Porosity, particle size, and postsynthetic treatment (calcination/solvent extraction) may be other significant contributors. The porosity effect is mainly connected to the increase or decrease in available surface area and postsynthetic treatment giving rise to different degrees of condensation and consequently biodegradation rate, possible residual template surfactants, as well as surface density of silanol groups. The latter has been especially brought forward in terms of hemocompatibility, whereby the silanol groups have been found to interact specifically with surface phospholipids on the red blood cell membranes. This effect was moreover enhanced by a higher density of surface silanols on nonporous silica surfaces as compared with corresponding porous surfaces, giving rise to a higher accessible surface, giving rise to a higher accessible external surface area, ultimately leading to hemolysis. Blocking the access to the silanol groups by functionalization with organic groups, however, diminished the observed hemolysis. Remarkably enough, primary amine groups were also very (and almost equally as PEG) effective in preventing hemolysis in a dose-dependent manner, even though the common conception is that positively charged

groups would enhance the interaction with the negatively charged cell membrane. The favourable effect of surface functionalization on biocompatibility also seems to be reflected in some of the existing biocompatibility studies, whereby the disadvantageous observations especially *in vivo* have pronouncedly been recorded for nonfunctionalized silicas. Whereas 240 mg/kg nonmodified MSNs resulted in immediate death when injected *iv.* into mice, the lethal dose (LD50) value for mesoporous hollow silica nanoparticles was found to be greater than 1000 mg/kg. These discrepancies have also been observed for the same type of materials when either solvent-extracted or calcined, whereby the extracted materials were found to inhibit cellular respiration, whereas the calcined counterparts were later shown to be reasonably biocompatible in terms of interference on bioenergetics when incubated at high concentrations (200 µg/ml) with murine tissues. One main contributing factor was also thought to be the surface density of silanol groups, as well as differences in accessible surface area between the studied materials possessing different pore sizes (~3 and ~7 nm, respectively). Similar findings have also been appointed for non-mesoporous silicas (as well as references therein). A disadvantage for the calcined MSNs could be the consequently lower hydrophilicity, arising from the lower density of silanols, potentially leading to poorer dispersibility under physiological conditions. Once dispersible MSNs have been successfully produced, however, surface functionalization can facilitate the dispersibility of the nanoparticulate carriers in the physiological environment. Another concern that must be solved, originated from metabolic changes caused by MSNs, resulting in melanoma promotion. It was suggested that the effect induced by MSNs was due to the decrease of endogenous reactive oxygen species in cells and upregulation of antiapoptotic molecules. These results show that tumor growth can be regulated by nanocarriers themselves in a reactive oxygen species-dependent manner, and this important finding highlights the need for more tests aiming at a clearer understanding of metabolic deviations in MSN-targeted cells.

2.9 Formulation Optimization

There are several steps for optimization of drug delivery systems (DDS) with design of experiment (DoE). Broadly, in seven salient phases, these stages can be summarized sequentially.

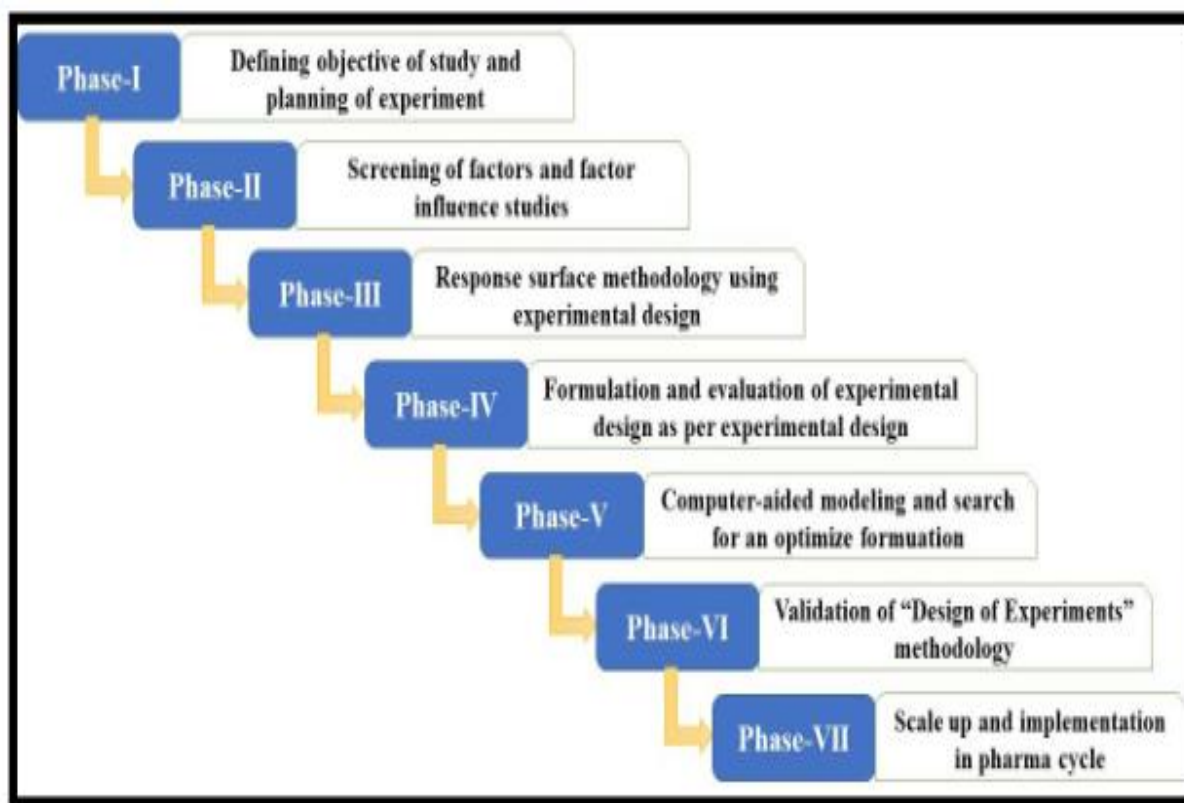


Figure 2.12 Seven-phase ladder for optimizing drug delivery systems

2.9.1 Experimental Designs

The twin basic features of the general scientific approach are the execution of the experiment and the resulting analysis of its experimental outcome (160). Only if the experiments are carried out in a systematic manner, the inferences of the change are predictable. Numerous forms of experimental designs exist. Various widely employed experimental designs for RSM, sampling, and factor-influence trials in pharmaceutical product development area (161).

- I. Factorial design
- II. Fractional factorial design
- III. Plackett-Burman design
- IV. Star designs
- V. Central composite design
- VI. Box-Behnken design
- VII. Center of gravity design

- VIII. Equi-radial design
- IX. Mixture design
- X. Taguchi design
- XI. Optimal design
- XII. Recht-schaffner design
- XIII. Cotter design

For three-factor analysis, an experimental architecture can inevitably be envisaged as a "cube," with the potential configurations of the factor levels (low or high) represented at its respective corners. Therefore, the cube could be the most fitting depiction of the experimental area being studied. Therefore, most forms discussed here are pictorially represented using this cubic model, with experimental points at the edges, centers of faces, edge centers, and so on. Such representation makes it easier to grasp different styles and similarities between them (162). The same definition is true to designs in which more than three parameters are modified, so that the hypercube reflects the experimental area. These cubic designs are common because to conceptualize and visualize the model, they are symmetrical and straightforward(163).

2.9.2 Design Augmentation

In the whole DoE , a condition often exists in which an analysis performed at some point is insufficient and must be further studied, or where it is appropriate to reuse the study carried out during the initial stages. It is possible to upgrade the former primitive design to a more modern design that offers more details, improved reliability and higher resolution. By introducing several more logical design points, this method of expansion of a statistical design is known as design augmentation. For e.g., by adding several further design points, a design following notable at two levels may be increased to a three-level design. It is possible to increase a design in a variety of ways, such as by replicating, applying core points to two-level structures, adding axial points (i.e., design points at multiple axes of the experimental region) or folding over (164).

2.9.3 Response surface

For a series of experiments conducted in a structured way to build a statistical model, one or more chosen experimental responses are reported during this critical stage in DoE. These methods include the postulation, with each response, of an analytical mathematical model that accurately reflects a shift in the response within the region of interest. Response

surface modelling (RSM) includes integrating the coefficients into the model equation of a specific response variable rather than calculating the results of each variable directly, and projecting the response in the form of a surface over the entire experimental domain (165).

RSM is primarily a group of mathematical strategies for the development of analytical models and the exploitation of models. It attempts to connect a response to a variety of predictors influencing it by careful design and study of experiments by creating a response surface, which is an area of space. The independent variables representing the relationship of these factors to the measured response are described within the upper and lower thresholds (166).

Response surface designs are experimental designs that allow the calculation of direct parameters, relative influence, and perhaps even quadratic effects and thus, give an understanding of the local form of response surface being investigated. In such conditions, it may be reasonable to characterize a response surface in a model that includes only significant interaction effects. These conditions emerge where no proof of "pure quadratic" curvature in the response of interest is revealed in the examination of the data - i.e., the response at the middle is nearly equal to the median response at the two severe stages, +1 and -1.

The value of the response rises from the bottom of the figure to the top of each section of Figure 2-13 and those of the factor settings rise from left to right. If a reaction behaves as in Figure 2-13(a), only variables with two levels - low and high - ought to be used in the design matrix to measure the action. This paradigm is a fundamental precept in basic designs for two-level scanning or factor effect. The minimal number of levels needed for a factor to measure its action is three if an answer behaves as in Figure 2-13(b).

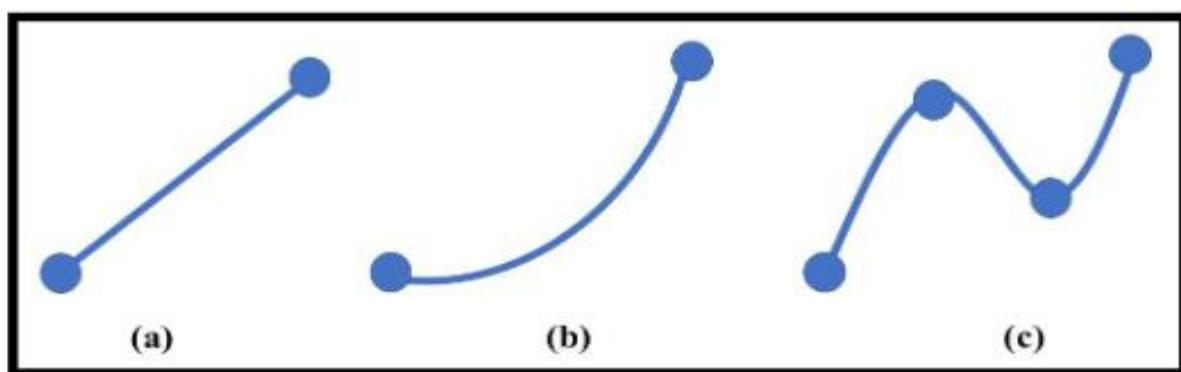


Figure 2.13 Different types of responses as a function of factor setting a) Linear b) Quadratic and c) Cubic

At this point, the addition of center points to a two-level architecture seems to be a sensible measure, but the layout of treatments in such a matrix can confuse all quadratic effects with one another. Only the quadratic aspect of the reaction can be detected by a two-level configuration with center points, but the actual pure quadratic results cannot be calculated. Quadratic structures for the development of drug delivery devices are commonly proposed. For DoE optimal protection, reaction surface designs containing experiments at three or more than three stages are also used. These reaction surface designs are used to define enhanced or optimal process conditions, address process issues and weak points, and render a more stable (i.e., less variable) formulation or process towards external and non-controllable influences. In pharmacy research, comparatively more complex cubic responses (Figure 2-10(c)) are very infrequent (165, 167, 168).

2.9.4 Mathematical models

An algebraic expression describing the dependency of a variable on the individual variable(s) is the mathematical model. Mathematical models can be conceptual or observational. An analytical model offers a way to identify the relationship of factor/response. Very commonly, but not necessarily, it is a set of polynomial function of a given order. The linear models most widely used are seen in following equations.

$$y = \beta_0 + \beta_1 X_1 + \beta_2 X_2 + \dots \quad (1)$$

$$y = \beta_0 + \beta_1 X_1 + \beta_2 X_2 + \beta_{12} X_1 X_2 + \dots \quad (2)$$

$$y = \beta_0 + \beta_1 X_1 + \beta_2 X_2 + \beta_{12} X_1 X_2 + \beta_{11} X_1^2 + \beta_{22} X_2^2 \dots + \varepsilon \dots \quad (3)$$

Where y reflects the approximate answer, often referred to as $E(y)$. The terms X indicate the value of the variables, and the constants describing the intercept, first-order/first-degree terms coefficients, second-order quadratic terms coefficients, and second-order interaction terms coefficients are β_0 , β_i , β_{ii} and β_{ij} . Pure errors are indicated by the symbol. Equations (1) and (2) are linear variables, representing, in 3-D space, a smooth surface and a twisted plane. Equation (3) is a linear second-order construct representing a curved, twisted plane resulting from quadratic terminology. There can also exist or be suggested a theoretical framework or mechanistic framework. Very frequently, it is a nonlinear model where it is typically not easy to transform to a linear function. However, such theoretical relationships are seldom used in the production of pharmaceutical products.

References

1. Lei S, Zheng R, Zhang S, Wang S, Chen R, Sun K, et al. Global patterns of breast cancer incidence and mortality: A population-based cancer registry data analysis from 2000 to 2020. *Cancer Communications*. 2021;41(11):1183-94.
2. Sung H, Ferlay J, Siegel RL, Laversanne M, Soerjomataram I, Jemal A, et al. Global Cancer Statistics 2020: GLOBOCAN Estimates of Incidence and Mortality Worldwide for 36 Cancers in 185 Countries. *CA: A Cancer Journal for Clinicians*. 2021;71(3):209-49.
3. Sopik V. International variation in breast cancer incidence and mortality in young women. *Breast Cancer Research and Treatment*. 2021;186(2):497-507.
4. Abd-Elnaby M, Alfonse M, Roushdy M. Classification of breast cancer using microarray gene expression data: A survey. *Journal of Biomedical Informatics*. 2021;117:103764.
5. Gupta V, Vasudev M, Doegar A, Sambyal N. Breast cancer detection from histopathology images using modified residual neural networks. *Biocybernetics and Biomedical Engineering*. 2021;41(4):1272-87.
6. Britt KL, Cuzick J, Phillips K-A. Key steps for effective breast cancer prevention. *Nature Reviews Cancer*. 2020;20(8):417-36.
7. Hanker AB, Sudhan DR, Arteaga CL. Overcoming Endocrine Resistance in Breast Cancer. *Cancer Cell*. 2020;37(4):496-513.
8. Torre LA, Islami F, Siegel RL, Ward EM, Jemal A. Global Cancer in Women: Burden and Trends. *Cancer Epidemiology, Biomarkers & Prevention*. 2017;26(4):444-57.
9. Hemmatzadeh M, Mohammadi H, Jadidi-Niaragh F, Asghari F, Yousefi M. The role of oncomirs in the pathogenesis and treatment of breast cancer. *Biomedicine & Pharmacotherapy*. 2016;78:129-39.
10. Bosch A, Eroles P, Zaragoza R, Viña JR, Lluch A. Triple-negative breast cancer: Molecular features, pathogenesis, treatment and current lines of research. *Cancer Treatment Reviews*. 2010;36(3):206-15.
11. Russo J, Russo IH. Role of differentiation in the pathogenesis and prevention of breast cancer. *Endocrine-related cancer*. 1997;4(1):7-21.
12. Feng Y, Spezia M, Huang S, Yuan C, Zeng Z, Zhang L, et al. Breast cancer development and progression: Risk factors, cancer stem cells, signaling pathways, genomics, and molecular pathogenesis. *Genes & Diseases*. 2018;5(2):77-106.
13. Brook N, Brook E, Dharmarajan A, Dass CR, Chan A. Breast cancer bone metastases: pathogenesis and therapeutic targets. *The International Journal of Biochemistry & Cell Biology*. 2018;96:63-78.
14. King J, Mir H, Singh S. Chapter Four - Association of Cytokines and Chemokines in Pathogenesis of Breast Cancer. In: Lakshmanaswamy R, editor. *Progress in Molecular Biology and Translational Science*. 151: Academic Press; 2017. p. 113-36.
15. Thomas M, Kelly ED, Abraham J, Kruse M. Invasive lobular breast cancer: A review of pathogenesis, diagnosis, management, and future directions of early stage disease. *Seminars in Oncology*. 2019;46(2):121-32.

16. Caswell-Jin JL, Plevritis SK, Tian L, Cadham CJ, Xu C, Stout NK, et al. Change in Survival in Metastatic Breast Cancer with Treatment Advances: Meta-Analysis and Systematic Review. *JNCI Cancer Spectrum*. 2018;2(4):pky062.
17. Spiegel D, Kraemer H, Bloom J, Gottheil E. EFFECT OF PSYCHOSOCIAL TREATMENT ON SURVIVAL OF PATIENTS WITH METASTATIC BREAST CANCER. *The Lancet*. 1989;334(8668):888-91.
18. Gradishar WJ. Taxanes for the Treatment of Metastatic Breast Cancer. *Breast Cancer: Basic and Clinical Research*. 2012;6:BCBCR.S8205.
19. Bender CM, Sereika SM, Berga SL, Vogel VG, Brufsky AM, Paraska KK, et al. Cognitive impairment associated with adjuvant therapy in breast cancer. *Psycho-Oncology*. 2006;15(5):422-30.
20. Jabo B, Lin AC, Aljehani MA, Ji L, Morgan JW, Selleck MJ, et al. Impact of Breast Reconstruction on Time to Definitive Surgical Treatment, Adjuvant Therapy, and Breast Cancer Outcomes. *Annals of Surgical Oncology*. 2018;25(10):3096-105.
21. Jasra S, Anampa J. Anthracycline Use for Early Stage Breast Cancer in the Modern Era: a Review. *Current Treatment Options in Oncology*. 2018;19(6):30.
22. de Gregorio A, Janni W, Friedl TWP, Nitz U, Rack B, Schneeweiss A, et al. The impact of anthracyclines in intermediate and high-risk HER2-negative early breast cancer—a pooled analysis of the randomised clinical trials PlanB and SUCCESS C. *British Journal of Cancer*. 2022;126(12):1715-24.
23. Abotaleb M, Kubatka P, Caprnda M, Varghese E, Zolakova B, Zubor P, et al. Chemotherapeutic agents for the treatment of metastatic breast cancer: An update. *Biomedicine & Pharmacotherapy*. 2018;101:458-77.
24. Giuliano M, Schettini F, Rognoni C, Milani M, Jerusalem G, Bachelot T, et al. Endocrine treatment versus chemotherapy in postmenopausal women with hormone receptor-positive, HER2-negative, metastatic breast cancer: a systematic review and network meta-analysis. *The Lancet Oncology*. 2019;20(10):1360-9.
25. Bortolini Silveira A, Bidard F-C, Tanguy M-L, Girard E, Trédan O, Dubot C, et al. Multimodal liquid biopsy for early monitoring and outcome prediction of chemotherapy in metastatic breast cancer. *npj Breast Cancer*. 2021;7(1):115.
26. Mukohara T, Hosono A, Mimaki S, Nakayama A, Kusuhara S, Funasaka C, et al. Effects of Ado-Trastuzumab Emtansine and Fam-Trastuzumab Deruxtecan on Metastatic Breast Cancer Harboring HER2 Amplification and the L755S Mutation. *The Oncologist*. 2021;26(8):635-9.
27. Pegram MD, Bondarenko I, Zorzetto MMC, Hingmire S, Iwase H, Krivorotko PV, et al. PF-05280014 (a trastuzumab biosimilar) plus paclitaxel compared with reference trastuzumab plus paclitaxel for HER2-positive metastatic breast cancer: a randomised, double-blind study. *British Journal of Cancer*. 2019;120(2):172-82.
28. Bachelot T, Ciruelos E, Schneeweiss A, Puglisi F, Peretz-Yablonski T, Bondarenko I, et al. Preliminary safety and efficacy of first-line pertuzumab combined with trastuzumab and taxane therapy for HER2-positive locally recurrent or metastatic breast cancer (PERUSE). *Annals of Oncology*. 2019;30(5):766-73.

29. Francies FZ, Hull R, Khanyile R, Dlamini Z. Breast cancer in low-middle income countries: abnormality in splicing and lack of targeted treatment options. *Am J Cancer Res.* 2020;10(5):1568-91.
30. Noonan S, Pasa A, Fontana V, Caviglia S, Bonanni B, Costa A, et al. A Survey among Breast Cancer Specialists on the Low Uptake of Therapeutic Prevention with Tamoxifen or Raloxifene. *Cancer Prevention Research.* 2018;11(1):38-43.
31. Xu T, Ding W, Ji X, Ao X, Liu Y, Yu W, et al. Molecular mechanisms of ferroptosis and its role in cancer therapy. *Journal of Cellular and Molecular Medicine.* 2019;23(8):4900-12.
32. Yin L, Duan J-J, Bian X-W, Yu S-c. Triple-negative breast cancer molecular subtyping and treatment progress. *Breast Cancer Research.* 2020;22(1):61.
33. Dallavalle S, Dobričić V, Lazzarato L, Gazzano E, Machuqueiro M, Pajeva I, et al. Improvement of conventional anti-cancer drugs as new tools against multidrug resistant tumors. *Drug Resistance Updates.* 2020;50:100682.
34. Robey RW, Pluchino KM, Hall MD, Fojo AT, Bates SE, Gottesman MM. Revisiting the role of ABC transporters in multidrug-resistant cancer. *Nature Reviews Cancer.* 2018;18(7):452-64.
35. Liu R, Chen Y, Liu G, Li C, Song Y, Cao Z, et al. PI3K/AKT pathway as a key link modulates the multidrug resistance of cancers. *Cell Death & Disease.* 2020;11(9):797.
36. Rocca A, Maltoni R, Bravaccini S, Donati C, Andreis D. Clinical utility of fulvestrant in the treatment of breast cancer: a report on the emerging clinical evidence. *Cancer Manag Res.* 2018;10:3083-99.
37. Li J, Wang Z, Shao Z. Fulvestrant in the treatment of hormone receptor-positive/human epidermal growth factor receptor 2-negative advanced breast cancer: A review. *Cancer Medicine.* 2019;8(5):1943-57.
38. Perey L, Paridaens R, Hawle H, Zaman K, Nolé F, Wildiers H, et al. Clinical benefit of fulvestrant in postmenopausal women with advanced breast cancer and primary or acquired resistance to aromatase inhibitors: final results of phase II Swiss Group for Clinical Cancer Research Trial (SAKK 21/00). *Annals of Oncology.* 2007;18(1):64-9.
39. Zbieg JR, Liang J, Li J, Blake RA, Chang J, Friedman L, et al. Discovery of GNE-502 as an orally bioavailable and potent degrader for estrogen receptor positive breast cancer. *Bioorganic & Medicinal Chemistry Letters.* 2021;50:128335.
40. Ribas R, Pancholi S, Guest SK, Marangoni E, Gao Q, Thuleau A, et al. AKT Antagonist AZD5363 Influences Estrogen Receptor Function in Endocrine-Resistant Breast Cancer and Synergizes with Fulvestrant (ICI182780) In Vivo. *Molecular Cancer Therapeutics.* 2015;14(9):2035-48.
41. Spoerke JM, Gendreau S, Walter K, Qiu J, Wilson TR, Savage H, et al. Heterogeneity and clinical significance of ESR1 mutations in ER-positive metastatic breast cancer patients receiving fulvestrant. *Nature Communications.* 2016;7(1):11579.
42. Alves CL, Elias D, Lyng M, Bak M, Kirkegaard T, Lykkesfeldt AE, et al. High CDK6 Protects Cells from Fulvestrant-Mediated Apoptosis and is a Predictor of Resistance to Fulvestrant in Estrogen Receptor-Positive Metastatic Breast Cancer. *Clinical Cancer Research.* 2016;22(22):5514-26.

43. Hascicek C, Sengel-Turk CT, Gumustas M, Ozkan AS, Bakar F, Das-Evcimen N, et al. Fulvestrant-loaded polymer-based nanoparticles for local drug delivery: Preparation and in vitro characterization. *Journal of Drug Delivery Science and Technology*. 2017;40:73-82.
44. Purohit P, Brahmshatriya P, Goswami V. Development of orally bioavailable prodrugs of fulvestrant for the treatment of metastatic/advanced breast cancer. *Journal of Clinical Oncology*. 2021;39(15_suppl):e13027-e.
45. TECHNOLOGY XALMSa, inventor; WIPO, assignee. Method of manufacturing fulvestrant sustained-release microspheres CHINA2007 03-08-2007.
46. Park J, Thomas S, Zhong AY, Wolfe AR, Krings G, Terranova-Barberio M, et al. Local delivery of hormonal therapy with silastic tubing for prevention and treatment of breast cancer. *Scientific Reports*. 2018;8(1):92.
47. Nabholz J-M, Mouret-Reynier M-A, Durando X, Van Praagh I, Al-Sukhun S, Ferriere J-P, et al. Comparative review of anastrozole, letrozole and exemestane in the management of early breast cancer. *Expert Opinion on Pharmacotherapy*. 2009;10(9):1435-47.
48. Lønning PE, Paridaens R, Thürlimann B, Piscitelli G, di Salle E. Exemestane experience in breast cancer treatment. *The Journal of Steroid Biochemistry and Molecular Biology*. 1997;61(3):151-5.
49. Sobral AF, Amaral C, Correia-da-Silva G, Teixeira N. Unravelling exemestane: From biology to clinical prospects. *The Journal of Steroid Biochemistry and Molecular Biology*. 2016;163:1-11.
50. Amaral C, Augusto TV, Tavares-da-Silva E, Roleira FMF, Correia-da-Silva G, Teixeira N. Hormone-dependent breast cancer: Targeting autophagy and PI3K overcomes Exemestane-acquired resistance. *The Journal of Steroid Biochemistry and Molecular Biology*. 2018;183:51-61.
51. Chalasani P, Stopeck A, Clarke K, Livingston R. A Pilot Study of Estradiol Followed by Exemestane for Reversing Endocrine Resistance in Postmenopausal Women With Hormone Receptor-Positive Metastatic Breast Cancer. *The Oncologist*. 2014;19(11):1127-8.
52. Singh AK, Chaurasiya A, Singh M, Upadhyay SC, Mukherjee R, Khar RK. Exemestane Loaded Self-Microemulsifying Drug Delivery System (SMEDDS): Development and Optimization. *AAPS PharmSciTech*. 2008;9(2):628-34.
53. Hiremath PS, Soppimath KS, Betageri GV. Proliposomes of exemestane for improved oral delivery: Formulation and in vitro evaluation using PAMPA, Caco-2 and rat intestine. *International Journal of Pharmaceutics*. 2009;380(1):96-104.
54. Jukanti R, Sheela S, Bandari S, Veerareddy PR. Enhanced Bioavailability of Exemestane Via Proliposomes based Transdermal Delivery. *Journal of Pharmaceutical Sciences*. 2011;100(8):3208-22.
55. Rizwanullah M, Perwez A, Mir SR, Alam Rizvi MM, Amin S. Exemestane encapsulated polymer-lipid hybrid nanoparticles for improved efficacy against breast cancer: optimization, in vitro characterization and cell culture studies. *Nanotechnology*. 2021;32(41):415101.
56. Kaur S, Jena SK, Samal SK, Saini V, Sangamwar AT. Freeze dried solid dispersion of exemestane: A way to negate an aqueous solubility and oral bioavailability problems. *European Journal of Pharmaceutical Sciences*. 2017;107:54-61.

57. Eedara BB, Bandari S. Lipid-based dispersions of exemestane for improved dissolution rate and intestinal permeability: in vitro and ex vivo characterization. *Artificial Cells, Nanomedicine, and Biotechnology*. 2017;45(5):917-27.
58. Yavuz B, Bilensoy E, Vural İ, Şumnu M. Alternative oral exemestane formulation: Improved dissolution and permeation. *International Journal of Pharmaceutics*. 2010;398(1):137-45.
59. Musa MN, David SA-O, Zulkipli IA-O, Mahadi AH, Chakravarthi S, Rajabalaya RA-O. Development and evaluation of exemestane-loaded lyotropic liquid crystalline gel formulations. (2228-5652 (Print)).
60. Jayapal JJ, Dhanaraj S. Exemestane loaded alginate nanoparticles for cancer treatment: Formulation and in vitro evaluation. *International Journal of Biological Macromolecules*. 2017;105:416-21.
61. Li Z, Liu K, Sun P, Mei L, Hao T, Tian Y, et al. Poly(D, L-lactide-co-glycolide)/montmorillonite nanoparticles for improved oral delivery of exemestane. *Journal of Microencapsulation*. 2013;30(5):432-40.
62. Timur B, Yilmaz Usta D, Teksin ZS. Investigation of the Effect of Colloidal Structures Formed During Lipolysis of Lipid-Based Formulation on Exemestane Permeability Using the In Vitro Lipolysis-Permeation Model. JDDST-D-22-01412.
63. Ballout F, Habli Z, Rahal ON, Fatfat M, Gali-Muhtasib H. Thymoquinone-based nanotechnology for cancer therapy: promises and challenges. *Drug Discovery Today*. 2018;23(5):1089-98.
64. Qin J, Gong N, Liao Z, Zhang S, Timashev P, Huo S, et al. Recent progress in mitochondria-targeting-based nanotechnology for cancer treatment. *Nanoscale*. 2021;13(15):7108-18.
65. Tran P, Nguyen TN, Lee Y, Tran PN, Park J-SJTKJoP, Society POJotKP, et al. Docetaxel-loaded PLGA nanoparticles to increase pharmacological sensitivity in MDA-MB-231 and MCF-7 breast cancer cells. 2021;25(5):479-88.
66. Mirzavi F, Barati M, Vakili-Ghartavol R, Roshan MK, Mashreghi M, Soukhtanloo M, et al. Pegylated liposomal encapsulation improves the antitumor efficacy of combretastatin A4 in murine 4T1 triple-negative breast cancer model. 2022;613:121396.
67. Sadaquat H, Akhtar M, Nazir M, Ahmad R, Alvi Z, Akhtar N. Biodegradable and biocompatible polymeric nanoparticles for enhanced solubility and safe oral delivery of docetaxel: In vivo toxicity evaluation. *International Journal of Pharmaceutics*. 2021;598:120363.
68. Mandal B, Bhattacharjee H, Mittal N, Sah H, Balabathula P, Thoma LA, et al. Core-shell-type lipid-polymer hybrid nanoparticles as a drug delivery platform. *Nanomedicine: Nanotechnology, Biology and Medicine*. 2013;9(4):474-91.
69. Jose C, Amra K, Bhavsar C, Momin MM, Omri A. Polymeric lipid hybrid nanoparticles: properties and therapeutic applications. *Critical Reviews™ in Therapeutic Drug Carrier Systems*. 2018;35(6).
70. Sivadasan D, Sultan MH, Madkhali O, Almoshari Y, Thangavel N. Polymeric Lipid Hybrid Nanoparticles (PLNs) as Emerging Drug Delivery Platform—A Comprehensive Review of Their Properties, Preparation Methods, and Therapeutic Applications. *Pharmaceutics*. 2021;13(8):1291.

71. Lee S-M, Chen H, Dettmer CM, O'Halloran TV, Nguyen ST. Polymer-caged liposomes: a pH-responsive delivery system with high stability. *Journal of the American Chemical Society*. 2007;129(49):15096-7.
72. Date T, Nimbalkar V, Kamat J, Mittal A, Mahato RI, Chitkara D. Lipid-polymer hybrid nanocarriers for delivering cancer therapeutics. *Journal of controlled release*. 2018;271:60-73.
73. Soares DCF, Domingues SC, Viana DB, Tebaldi ML. Polymer-hybrid nanoparticles: Current advances in biomedical applications. *Biomedicine & Pharmacotherapy*. 2020;131:110695.
74. Liu Y, Xie X, Chen H, Hou X, He Y, Shen J, et al. Advances in next-generation lipid-polymer hybrid nanocarriers with emphasis on polymer-modified functional liposomes and cell-based-biomimetic nanocarriers for active ingredients and fractions from Chinese medicine delivery. *Nanomedicine: Nanotechnology, Biology and Medicine*. 2020;29:102237.
75. Mukherjee A, Waters AK, Kalyan P, Achrol AS, Kesari S, Yenugonda VM. Lipid-polymer hybrid nanoparticles as a next-generation drug delivery platform: state of the art, emerging technologies, and perspectives. *International journal of nanomedicine*. 2019;14:1937.
76. Szczęch M, Szczepanowicz K. Polymeric core-shell nanoparticles prepared by spontaneous emulsification solvent evaporation and functionalized by the layer-by-layer method. *Nanomaterials*. 2020;10(3):496.
77. Garg NK, Singh B, Sharma G, Kushwah V, Tyagi RK, Jain S, et al. Development and characterization of single step self-assembled lipid polymer hybrid nanoparticles for effective delivery of methotrexate. *RSC advances*. 2015;5(77):62989-99.
78. Yang T, Wang Y, Li Z, Dai W, Yin J, Liang L, et al. Targeted delivery of a combination therapy consisting of combretastatin A4 and low-dose doxorubicin against tumor neovasculature. *Nanomedicine: Nanotechnology, Biology and Medicine*. 2012;8(1):81-92.
79. Liang C, Li N, Cai Z, Liang R, Zheng X, Deng L, et al. Co-encapsulation of magnetic Fe₃O₄ nanoparticles and doxorubicin into biocompatible PLGA-PEG nanocarriers for early detection and treatment of tumours. *Artificial cells, nanomedicine, and biotechnology*. 2019;47(1):4211-21.
80. Yanasarn N, Sloat BR, Cui Z. Nanoparticles engineered from lecithin-in-water emulsions as a potential delivery system for docetaxel. *International journal of pharmaceutics*. 2009;379(1):174-80.
81. Gorain B, Choudhury H, Pandey M, Kesharwani P. Paclitaxel loaded vitamin E-TPGS nanoparticles for cancer therapy. *Materials Science and Engineering: C*. 2018;91:868-80.
82. Pereira S, Egbu R, Jannati G. Docetaxel-loaded liposomes: the effect of lipid composition and purification on drug encapsulation and in vitro toxicity. *International journal of pharmaceutics*. 2016;514(1):150-9.
83. Liu J, Cheng H, Han L, Qiang Z, Zhang X, Gao W, et al. Synergistic combination therapy of lung cancer using paclitaxel-and triptolide-coloated lipid-polymer hybrid nanoparticles. *Drug design, development and therapy*. 2018;12:3199.
84. Pandey SK, Halder C, Vishwas DK, Maiti P. S ynthesis and in vitro evaluation of melatonin entrapped PLA nanoparticles: A n oxidative stress and T-cell response using golden hamster. *Journal of Biomedical Materials Research Part A*. 2015;103(9):3034-44.

85. Deljoo S, Rabiee N, Rabiee M. Curcumin-hybrid nanoparticles in drug delivery system. *Asian Journal of Nanosciences and Materials*. 2019;2(1):66-91.
86. Wang W, Chen S, Zhang L, Wu X, Wang J, Chen J-F, et al. Poly (lactic acid)/chitosan hybrid nanoparticles for controlled release of anticancer drug. *Materials Science and Engineering: C*. 2015;46:514-20.
87. Pornpitchanarong C, Rojanarata T, Opanasopit P, Ngawhirunpat T, Patrojanasophon P. Catechol-modified chitosan/hyaluronic acid nanoparticles as a new avenue for local delivery of doxorubicin to oral cancer cells. *Colloids and Surfaces B: Biointerfaces*. 2020;196:111279.
88. Mandal B, Mittal NK, Balabathula P, Thoma LA, Wood GC. Development and in vitro evaluation of core-shell type lipid-polymer hybrid nanoparticles for the delivery of erlotinib in non-small cell lung cancer. *European journal of pharmaceutical sciences*. 2016;81:162-71.
89. Barkat A, Beg S, Panda SK, S Alharbi K, Rahman M, Ahmed FJ. Functionalized mesoporous silica nanoparticles in anticancer therapeutics. *Seminars in Cancer Biology*. 2021;69:365-75.
90. Lu J, Liong M, Zink JJ, Tamanoi F. Mesoporous Silica Nanoparticles as a Delivery System for Hydrophobic Anticancer Drugs. *Small*. 2007;3(8):1341-6.
91. Lin C-H, Cheng S-H, Liao W-N, Wei P-R, Sung P-J, Weng C-F, et al. Mesoporous silica nanoparticles for the improved anticancer efficacy of cis-platin. *International Journal of Pharmaceutics*. 2012;429(1):138-47.
92. Muñoz B, Rámila A, Pérez-Pariente J, Díaz I, Vallet-Regí M. MCM-41 Organic Modification as Drug Delivery Rate Regulator. *Chemistry of Materials*. 2003;15(2):500-3.
93. Lv X, Zhang L, Xing F, Lin H. Controlled synthesis of monodispersed mesoporous silica nanoparticles: Particle size tuning and formation mechanism investigation. *Microporous and Mesoporous Materials*. 2016;225:238-44.
94. Pal N, Lee J-H, Cho E-B. Recent Trends in Morphology-Controlled Synthesis and Application of Mesoporous Silica Nanoparticles. *Nanomaterials*. 2020;10(11).
95. Vazquez NI, Gonzalez Z, Ferrari B, Castro Y. Synthesis of mesoporous silica nanoparticles by sol-gel as nanocontainer for future drug delivery applications. *Boletín de la Sociedad Española de Cerámica y Vidrio*. 2017;56(3):139-45.
96. Slowing I, Trewyn BG, Lin VSY. Effect of Surface Functionalization of MCM-41-Type Mesoporous Silica Nanoparticles on the Endocytosis by Human Cancer Cells. *Journal of the American Chemical Society*. 2006;128(46):14792-3.
97. Kim T-W, Chung P-W, Lin VSY. Facile Synthesis of Monodisperse Spherical MCM-48 Mesoporous Silica Nanoparticles with Controlled Particle Size. *Chemistry of Materials*. 2010;22(17):5093-104.
98. Trewyn BG, Whitman CM, Lin VSY. Morphological Control of Room-Temperature Ionic Liquid Templated Mesoporous Silica Nanoparticles for Controlled Release of Antibacterial Agents. *Nano Letters*. 2004;4(11):2139-43.
99. Slowing II, Vivero-Escoto JL, Wu C-W, Lin VSY. Mesoporous silica nanoparticles as controlled release drug delivery and gene transfection carriers. *Advanced Drug Delivery Reviews*. 2008;60(11):1278-88.
100. Tao Z, Toms BB, Goodisman J, Asefa T. Mesoporosity and Functional Group Dependent Endocytosis and Cytotoxicity of Silica Nanomaterials. *Chemical Research in Toxicology*. 2009;22(11):1869-80.

101. de Barros ALB, de Oliveira Ferraz KS, Dantas TCS, Andrade GF, Cardoso VN, Sousa EMBd. Synthesis, characterization, and biodistribution studies of ^{99m}Tc-labeled SBA-16 mesoporous silica nanoparticles. *Materials Science and Engineering: C*. 2015;56:181-8.
102. Ma'mani L, Nikzad S, Kheiri-manjili H, al-Musawi S, Saeedi M, Askarlou S, et al. Curcumin-loaded guanidine functionalized PEGylated I3ad mesoporous silica nanoparticles KIT-6: Practical strategy for the breast cancer therapy. *European Journal of Medicinal Chemistry*. 2014;83:646-54.
103. Li H, Chen Y, Liu S, Liu Q. Enhancement of hydrothermal synthesis of FDU-12-derived nickel phyllosilicate using double accelerators of ammonium fluoride and urea for CO₂ methanation. *Journal of CO₂ Utilization*. 2021;52:101677.
104. Colmenares MG, Simon U, Schmidt F, Dey S, Schmidt J, Thomas A, et al. Tailoring of ordered mesoporous silica COK-12: Room temperature synthesis of mesocellular foam and multilamellar vesicles. *Microporous and Mesoporous Materials*. 2018;267:142-9.
105. Liu S-H, Chen S-C. Stepwise synthesis, characterization, and electrochemical properties of ordered mesoporous carbons containing well-dispersed Pt nanoparticles using a functionalized template route. *Journal of Solid State Chemistry*. 2011;184(9):2420-7.
106. Slowing II, Vivero-Escoto JL, Trewyn BG, Lin VSY. Mesoporous silica nanoparticles: structural design and applications. *Journal of Materials Chemistry*. 2010;20(37):7924-37.
107. Kumar S, Malik MM, Purohit R. Synthesis Methods of Mesoporous Silica Materials. *Materials Today: Proceedings*. 2017;4(2, Part A):350-7.
108. Bao M, Zhu G, Wang L, Wang M, Gao C. Preparation of monodispersed spherical mesoporous nanosilica-polyamide thin film composite reverse osmosis membranes via interfacial polymerization. *Desalination*. 2013;309:261-6.
109. Chen H, Yang H, Xi Y. Highly ordered and hexagonal mesoporous silica materials with large specific surface from natural rectorite mineral. *Microporous and Mesoporous Materials*. 2019;279:53-60.
110. Mohamad DF, Osman NS, Nazri MKHM, Mazlan AA, Hanafi MF, Esa YAM, et al. Synthesis of Mesoporous Silica Nanoparticle from Banana Peel Ash for Removal of Phenol and Methyl Orange in Aqueous Solution. *Materials Today: Proceedings*. 2019;19:1119-25.
111. Kamarudin NHN, Jalil AA, Triwahyono S, Artika V, Salleh NFM, Karim AH, et al. Variation of the crystal growth of mesoporous silica nanoparticles and the evaluation to ibuprofen loading and release. *Journal of Colloid and Interface Science*. 2014;421:6-13.
112. Sun J-G, Jiang Q, Zhang X-P, Shan K, Liu B-H, Zhao C, et al. Mesoporous silica nanoparticles as a delivery system for improving antiangiogenic therapy. *International journal of nanomedicine*. 2019;14:1489-501.
113. Ikari K, Suzuki K, Imai H. Structural Control of Mesoporous Silica Nanoparticles in a Binary Surfactant System. *Langmuir*. 2006;22(2):802-6.
114. Zhang J, Li X, Rosenholm JM, Gu H-c. Synthesis and characterization of pore size-tunable magnetic mesoporous silica nanoparticles. *Journal of Colloid and Interface Science*. 2011;361(1):16-24.
115. Chiang Y-D, Lian H-Y, Leo S-Y, Wang S-G, Yamauchi Y, Wu KCW. Controlling Particle Size and Structural Properties of Mesoporous Silica Nanoparticles Using the Taguchi Method. *The Journal of Physical Chemistry C*. 2011;115(27):13158-65.

116. Vanichvattanadecha C, Singhapong W, Jaroenworuluck A. Different sources of silicon precursors influencing on surface characteristics and pore morphologies of mesoporous silica nanoparticles. *Applied Surface Science*. 2020;513:145568.
117. Zhou C, Yan C, Zhao J, Wang H, Zhou Q, Luo W. Rapid synthesis of morphology-controlled mesoporous silica nanoparticles from silica fume. *Journal of the Taiwan Institute of Chemical Engineers*. 2016;62:307-12.
118. Tsou M-H, Lee C-C, Wu Z-Y, Lee Z-H, Lin H-M. Mesoporous silica nanoparticles with fluorescent and magnetic dual-imaging properties to deliver fucoidan. *International Journal of Biological Macromolecules*. 2021;188:870-8.
119. Wu KCW, Yamauchi Y. Controlling physical features of mesoporous silica nanoparticles (MSNs) for emerging applications. *Journal of Materials Chemistry*. 2012;22(4):1251-6.
120. Li Z, Zhang Y, Feng N. Mesoporous silica nanoparticles: synthesis, classification, drug loading, pharmacokinetics, biocompatibility, and application in drug delivery. *Expert Opinion on Drug Delivery*. 2019;16(3):219-37.
121. Qian KK, Bogner RH. Application of Mesoporous Silicon Dioxide and Silicate in Oral Amorphous Drug Delivery Systems. *Journal of Pharmaceutical Sciences*. 2012;101(2):444-63.
122. Vivero-Escoto JL, Huxford-Phillips RC, Lin W. Silica-Based Nanoprobes for Biomedical Imaging and Theranostic Applications. *Chem Soc Rev*. 2012;41:2673.
123. Tao Z, Toms B, Goodisman J, Asefa T. Mesoporous Silica Microparticles Enhance the Cytotoxicity of Anticancer Platinum Drugs. *ACS Nano*. 2010;4:789.
124. Meng H, Liong M, Xia T, Li Z, Ji Z, Zink JJ, et al. Engineered Design of Mesoporous Silica Nanoparticles to Deliver Doxorubicin and P-Glycoprotein siRNA to Overcome Drug Resistance in a Cancer Cell Line. *ACS Nano*. 2010;4:4539.
125. Castillo RR, Colilla M, Vallet-Regí M. Advances in Mesoporous Silica-Based Nanocarriers for Co-delivery and Combination Therapy Against Cancer. *Expert Opin Drug Delivery*. 2017;14:229.
126. Castillo RR, Baeza A, Vallet-Regí M. Recent Applications of the Combination of Mesoporous Silica Nanoparticles with Nucleic Acids: Development of Bioresponsive Devices, Carriers and Sensors. *Biomater Sci*. 2017;5:353.
127. Farjadian F, Roointan A, Mohammadi-Samani S, Hosseini M. Mesoporous silica nanoparticles: Synthesis, pharmaceutical applications, biodistribution, and biosafety assessment. *Chemical Engineering Journal*. 2019;359:684-705.
128. Zhou Y, Quan G, Wu Q, Zhang X, Niu B, Wu B, et al. Mesoporous Silica Nanoparticles for Drug and Gene Delivery. *Acta Pharm Sin B*. 2018;8:165.
129. Akram Z, Daood U, Aati S, Ngo H, Fawzy AS. Formulation of pH-sensitive chlorhexidine-loaded/mesoporous silica nanoparticles modified experimental dentin adhesive. *Materials Science and Engineering: C*. 2021;122:111894.
130. Li T, Shi S, Goel S, Shen X, Xie X, Chen Z, et al. Recent advancements in mesoporous silica nanoparticles towards therapeutic applications for cancer. *Acta Biomaterialia*. 2019;89:1-13.
131. Chiu H-Y, Göbl D, Haddick L, Engelke H, Bein T. Clickable Multifunctional Large-Pore Mesoporous Silica Nanoparticles as Nanocarriers. *Chemistry of Materials*. 2018;30(3):644-54.

132. Wu S-H, Mou C-Y, Lin H-P. Synthesis of mesoporous silica nanoparticles. *Chemical Society Reviews*. 2013;42(9):3862-75.
133. Möller K, Bein T. Talented Mesoporous Silica Nanoparticles. *Chemistry of Materials*. 2017;29(1):371-88.
134. Chen F, Hong H, Shi S, Goel S, Valdovinos HF, Hernandez R, et al. Engineering of Hollow Mesoporous Silica Nanoparticles for Remarkably Enhanced Tumor Active Targeting Efficacy. *Scientific Reports*. 2014;4(1):5080.
135. Dehghani S, Danesh NM, Ramezani M, Alibolandi M, Lavaee P, Nejabat M, et al. A label-free fluorescent aptasensor for detection of kanamycin based on dsDNA-capped mesoporous silica nanoparticles and Rhodamine B. *Analytica Chimica Acta*. 2018;1030:142-7.
136. Zhang J, Sun Y, Tian B, Li K, Wang L, Liang Y, et al. Multifunctional mesoporous silica nanoparticles modified with tumor-shedable hyaluronic acid as carriers for doxorubicin. *Colloids and Surfaces B: Biointerfaces*. 2016;144:293-302.
137. Xie M, Shi H, Li Z, Shen H, Ma K, Li B, et al. A multifunctional mesoporous silica nanocomposite for targeted delivery, controlled release of doxorubicin and bioimaging. *Colloids and Surfaces B: Biointerfaces*. 2013;110:138-47.
138. Xie X, Li F, Zhang H, Lu Y, Lian S, Lin H, et al. EpCAM aptamer-functionalized mesoporous silica nanoparticles for efficient colon cancer cell-targeted drug delivery. *European Journal of Pharmaceutical Sciences*. 2016;83:28-35.
139. Chen F, Goel S, Valdovinos HF, Luo H, Hernandez R, Barnhart TE, et al. In Vivo Integrity and Biological Fate of Chelator-Free Zirconium-89-Labeled Mesoporous Silica Nanoparticles. *ACS Nano*. 2015;9(8):7950-9.
140. Vaikari VP, Park M, Keossayan L, MacKay JA, Alachkar H. Anti-CD99 scFv-ELP nanoworms for the treatment of acute myeloid leukemia. *Nanomedicine: Nanotechnology, Biology and Medicine*. 2020;29:102236.
141. Liao Y-T, Liu C-H, Yu J, Wu KCW. Liver cancer cells: targeting and prolonged-release drug carriers consisting of mesoporous silica nanoparticles and alginate microspheres. *International journal of nanomedicine*. 2014;9:2767-78.
142. Quan G, Pan X, Wang Z, Wu Q, Li G, Dian L, et al. Lactosaminated mesoporous silica nanoparticles for asialoglycoprotein receptor targeted anticancer drug delivery. *Journal of Nanobiotechnology*. 2015;13(1):7.
143. Dai L, Wei D, Zhang J, Shen T, Zhao Y, Liang J, et al. Aptamer-conjugated mesoporous polydopamine for docetaxel targeted delivery and synergistic photothermal therapy of prostate cancer. *Cell Proliferation*. 2021;54(11):e13130.
144. Feng Y, Panwar N, Tng DJH, Tjin SC, Wang K, Yong K-T. The application of mesoporous silica nanoparticle family in cancer theranostics. *Coordination Chemistry Reviews*. 2016;319:86-109.
145. Mendiratta S, Hussein M, Nasser HA, Ali AAA. Multidisciplinary Role of Mesoporous Silica Nanoparticles in Brain Regeneration and Cancers: From Crossing the Blood–Brain Barrier to Treatment. *Particle & Particle Systems Characterization*. 2019;36(9):1900195.
146. Wu X, Han Z, Schur RM, Lu Z-R. Targeted Mesoporous Silica Nanoparticles Delivering Arsenic Trioxide with Environment Sensitive Drug Release for Effective Treatment

- of Triple Negative Breast Cancer. *ACS Biomaterials Science & Engineering*. 2016;2(4):501-7.
147. Li X, Wu M, Pan L, Shi J. Tumor vascular-targeted co-delivery of anti-angiogenesis and chemotherapeutic agents by mesoporous silica nanoparticle-based drug delivery system for synergetic therapy of tumor. *International journal of nanomedicine*. 2015;11:93-105.
148. Karimi MH, Mahdavinia GR, Massoumi B. pH-controlled sunitinib anticancer release from magnetic chitosan nanoparticles crosslinked with κ -carrageenan. *Materials Science and Engineering: C*. 2018;91:705-14.
149. Wang K, Yao H, Meng Y, Wang Y, Yan X, Huang R. Specific aptamer-conjugated mesoporous silica-carbon nanoparticles for HER2-targeted chemo-photothermal combined therapy. *Acta Biomaterialia*. 2015;16:196-205.
150. Chen F, Hong H, Zhang Y, Valdovinos HF, Shi S, Kwon GS, et al. In Vivo Tumor Targeting and Image-Guided Drug Delivery with Antibody-Conjugated, Radiolabeled Mesoporous Silica Nanoparticles. *ACS Nano*. 2013;7(10):9027-39.
151. Han L, Tang C, Yin C. Dual-targeting and pH/redox-responsive multi-layered nanocomplexes for smart co-delivery of doxorubicin and siRNA. *Biomaterials*. 2015;60:42-52.
152. Zhang J, Wang X, Wen J, Su X, Weng L, Wang C, et al. Size effect of mesoporous organosilica nanoparticles on tumor penetration and accumulation. *Biomaterials Science*. 2019;7(11):4790-9.
153. Rong L, Qin S-Y, Zhang C, Cheng Y-J, Feng J, Wang S-B, et al. Biomedical applications of functional peptides in nano-systems. *Materials Today Chemistry*. 2018;9:91-102.
154. Xiong L, Du X, Kleitz F, Qiao SZ. Cancer-Cell-Specific Nuclear-Targeted Drug Delivery by Dual-Ligand-Modified Mesoporous Silica Nanoparticles. *Small*. 2015;11(44):5919-26.
155. Yu B, Zhou Y, Song M, Xue Y, Cai N, Luo X, et al. Synthesis of selenium nanoparticles with mesoporous silica drug-carrier shell for programmed responsive tumor targeted synergistic therapy. *RSC Advances*. 2016;6(3):2171-5.
156. Morshed RA, Muroski ME, Dai Q, Wegscheid ML, Auffinger B, Yu D, et al. Cell-Penetrating Peptide-Modified Gold Nanoparticles for the Delivery of Doxorubicin to Brain Metastatic Breast Cancer. *Molecular Pharmaceutics*. 2016;13(6):1843-54.
157. Colilla M, Vallet-Regí M. Targeted Stimuli-Responsive Mesoporous Silica Nanoparticles for Bacterial Infection Treatment. *International Journal of Molecular Sciences*. 2020;21(22).
158. Cheng Y-J, Qin S-Y, Ma Y-H, Chen X-S, Zhang A-Q, Zhang X-Z. Super-pH-Sensitive Mesoporous Silica Nanoparticle-Based Drug Delivery System for Effective Combination Cancer Therapy. *ACS Biomaterials Science & Engineering*. 2019;5(4):1878-86.
159. Cheng K, Zhang Y, Li Y, Gao Z, Chen F, Sun K, et al. A novel pH-responsive hollow mesoporous silica nanoparticle (HMSN) system encapsulating doxorubicin (DOX) and glucose oxidase (GOX) for potential cancer treatment. *Journal of Materials Chemistry B*. 2019;7(20):3291-302.
160. Tavares Luiz M, Santos Rosa Viegas J, Palma Abriata J, Viegas F, Testa Moura de Carvalho Vicentini F, Lopes Badra Bentley MV, et al. Design of experiments (DoE) to develop

and to optimize nanoparticles as drug delivery systems. *European Journal of Pharmaceutics and Biopharmaceutics*. 2021;165:127-48.

161. Choi J-S, Park J-S. *J JoBM*. Design and evaluation of the anticancer activity of paclitaxel-loaded anisotropic-poly (lactic-co-glycolic acid) nanoparticles with PEGylated chitosan surface modifications. 2020;162:1064-75.

162. Moolakkadath T, Aqil M, Ahad A, Imam SS, Iqbal B, Sultana Y, et al. Development of transthesomes formulation for dermal fisetin delivery: Box–Behnken design, optimization, in vitro skin penetration, vesicles–skin interaction and dermatokinetic studies. *Artificial cells, nanomedicine, and biotechnology*. 2018;46(sup2):755-65.

163. Xiong Y, Guo D, Wang L, Zheng X, Zhang Y, Chen J. Development of nobiliside A loaded liposomal formulation using response surface methodology. *International journal of pharmaceutics*. 2009;371(1-2):197-203.

164. Lucas JM. *Response Surface Methodology: Process and Product Optimization Using Designed Experiments*, 3rd edition. *Journal of Quality Technology*. 2010;42(2):228-30.

165. Peng X, Yang G, Shi Y, Zhou Y, Zhang M, Li S. Box–Behnken design based statistical modeling for the extraction and physicochemical properties of pectin from sunflower heads and the comparison with commercial low-methoxyl pectin. *Scientific Reports*. 2020;10(1):3595.

166. Barabadi H, Honary S, Ebrahimi P, Alizadeh A, Naghibi F, Saravanan M. Optimization of myco-synthesized silver nanoparticles by response surface methodology employing Box–Behnken design. *Inorganic and Nano-Metal Chemistry*. 2019;49(2):33-43.

167. Prakash Maran J, Manikandan S, Thirugnanasambandham K, Vigna Nivetha C, Dinesh R. Box–Behnken design based statistical modeling for ultrasound-assisted extraction of corn silk polysaccharide. *Carbohydrate Polymers*. 2013;92(1):604-11.

168. Draper NR, Lin DKJ. 11 Response surface designs. *Handbook of Statistics*. 13: Elsevier; 1996. p. 343-75.